

**KA-BAND TRANSMITTER
FOR
IP TRANSFER OVER SATELLITE**

by

Saša T. Trajković
B.A.Sc., University of Belgrade, 1988

PROJECT SUBMITTED IN PARTIAL FULFILLMENT OF
THE REQUIREMENTS FOR THE DEGREE OF
MASTER OF ENGINEERING

in the School
of
Engineering Science

© Saša Trajković 2002
SIMON FRASER UNIVERSITY
April 2002

All rights reserved. This work may not be
reproduced in whole or in part, by photocopy
or other means, without permission of the author.

APPROVAL

Name: Sasa T. Trajkovic
Degree: Master of Engineering
Title of thesis: KA-BAND TRANSMITTER FOR IP TRANSFER OVER
SATELLITE

Examining Committee:

Chair: Dr. Ash Parameswaran

~~Dr. Shawn Stapleton, P.Eng.
Senior Supervisor~~

~~Dr. Ljiljana Trajkovic
Supervisor~~

Date approved: April 2, 2002

PARTIAL COPYRIGHT LICENSE

I hereby grant to Simon Fraser University the right to lend my thesis, project or extended essay (the title of which is shown below) to users of the Simon Fraser University Library, and to make partial or single copies only for such users or in response to a request from the library of any other university, or other educational institution, on its own behalf or for one of its users. I further agree that permission for multiple copying of this work for scholarly purposes may be granted by me or the Dean of Graduate Studies. It is understood that copying or publication of this work for financial gain shall not be allowed without my written permission.

Title of Thesis/Project/Extended Essay

KA-BAND TRANSMITTER FOR IP TRANSFER OVER SATELLITE

Author:

(signature) _____

(name) SASA TRAJKOVIC

(date) April 11 / 2002

ABSTRACT

This project presents a single conversion, no spectral inversion, Ka-band transmitter. The transmitter is part of a satellite interactive terminal used in a new generation of interactive networks for Internet protocol transfer over Ka-band satellites. The Ka-band transmitter is a part of the return channel link, for data transport from customer sites, over satellite, to the Hub that is connected to the Internet backbone.

Design considerations and simulation results for the transmitter upconverter section only are presented. Measurements performed on sub-circuit level show a very close match between the simulation data and actual measurement results. Unit level measurement is also completed, and results illustrate that the transmitter exceeds the required specification with a considerable margin.

The return channel link budget calculation is carried out with a goal to determine whether or not the required probability of error performance is met with a data transfer rate of 348 Kbps. This calculation demonstrates that an availability of service of 99.7% can be achieved when this transmitter/outdoor unit is deployed in the ASTRA Broad-band interactive network.

DEDICATION

To my mother and sister,

and

my wife Snezana

ACKNOWLEDGMENTS

I would like to thank my supervisor Dr. Shawn Stapleton for all the help and guidance.

Also, my wife Snezana deserves a big credit for her understanding, encouragement and help during my work on this project.

Finally, special thanks to my dear colleagues from Norsat – Dr. Amiee Chan, Beven Kocay, Pieter Bezuidenhout, and all the others for their constant support and help.

TABLE OF CONTENTS

APPROVAL	ii
ABSTRACT	iii
DEDICATION	iv
ACKNOWLEDGMENTS	v
TABLE OF CONTENTS	vi
LIST OF TABLES	vii
LIST OF FIGURES	viii
1 INTRODUCTION	1
2 BACKGROUND	2
2.1 Internet Over Satellite.....	2
2.1.1 Historical Review	2
2.1.2 Internet Applications	3
2.2 Geostationary Satellite Networks	6
2.2.1 Review of Current Geostationary Satellite Networks.....	7
2.2.2 Ka-band Satellite Networks.....	12
3 SATELLITE INTERACTIVE TERMINAL	19
3.1 General Description	19
3.2 Outdoor Unit Overview	21
3.3 Ka-band Transmitter	25
3.3.1 Block Diagram	27
3.3.2 Up-converter Circuitry Description	28
3.4 Measurement Results	49
3.4.1 Sub-circuit Level Measurement Results.....	49
3.4.2 Unit Level Measurement Results	60
4 RETURN CHANNEL LINK BUDGET CALCULATION	66
4.1 Introduction.....	66

4.2 Link Budget.....	66
5 CONCLUSION	72
REFERENCES	73

LIST OF TABLES

Table 1: Internet applications grouped by commonly used protocols.....	5
Table 2: Comparison table of geostationary satellite networks.	18
Table 3: Main parameters of the outdoor unit.....	22
Table 4: Properties of the different outdoor units.....	23
Table 5: Main electrical and mechanical parameters of the Ka-band transmitter.	25
Table 6: Measurement results collected using automated measurement setup.....	65
Table 7: Link budget calculation for clear sky and 0.3% rain rate exceeded conditions.	68

LIST OF FIGURES

Figure 1: Internet network topology.....	4
Figure 2: Dedicated single channel per carrier satellite network topology.....	7
Figure 3: Very small aperture terminal satellite network topology.....	9
Figure 4: Demand assigned multiple access satellite network topology.....	11
Figure 5: Hot Bird 6 satellite Ka-band uplink coverage.....	14
Figure 6: Hot Bird 6 satellite Ka-band downlink coverage.....	14
Figure 7: ASTRA broadband interactive network for IP transfer over Ka-band satellite.	16
Figure 8: ASTRA network return link frequency plan.....	17
Figure 9: Block diagram of the satellite interactive terminal.....	20
Figure 10: Block diagram of the outdoor unit.....	21
Figure 11: Norsat outdoor unit with 76 cm Gregorian dual offset parabola antenna system, transmitter and receiver with feed/diplexer.....	24
Figure 12: Norsat outdoor unit – boom arm assembly detail.....	24
Figure 13: Simplified block diagram of the Ka-band transmitter.....	27
Figure 14: Frequency spectrum content presentation at the different points of the up- converter chain.....	29
Figure 15: Block diagram of the intermediate frequency section.....	29
Figure 16: Schematic diagram of the diplexer stage.....	30
Figure 17: Schematic diagram of the attenuator ATT1.....	31
Figure 18: Schematic diagram of the low-pass filter LP1 with lumped elements.....	32
Figure 19: Schematic diagram of the low-pass filter LP1 with distributed elements.....	32
Figure 20: Simulated return loss and S21 transfer characteristics of the low-pass filter LP1.....	33
Figure 21: Schematic diagram of the high-pass filter HP1 with lumped elements.....	34
Figure 22: Schematic diagram of the high-pass filter with distributed elements.....	35
Figure 23: Simulated return loss and S21 transfer characteristics of the high-pass filter HP1.....	35
Figure 24: Schematic diagram of the MMIC amplifier A1 and biasing circuitry.....	36

Figure 25: Simulated input/output return loss and S21 transfer characteristics of the amplifier A1.	38
Figure 26: Schematic diagram of the band-pass shunt nonconstant-impedance type amplitude equalizer.	39
Figure 27: Simulated input/output return loss and S21 transfer characteristics of the equalizer stage with resonant frequency set to 3 GHz.	39
Figure 28: Simulated input/output return loss and S21 transfer characteristics of the amplifier A2.	40
Figure 29: Simulated input/output return loss and S21 transfer characteristics of the intermediate frequency stage.....	41
Figure 30: Block diagram of the resistive FET mixer.	42
Figure 31: Schematic diagram of the resistive FET mixer.	43
Figure 32: Simulated mixer RF output power as a function of RF frequency.	44
Figure 33: Simulated mixer conversion loss as a function of IF frequency.....	44
Figure 34: Simulated mixer compression characteristic – output RF power as a function of input IF power.....	45
Figure 35: Simulated input impedances of the IF, LO and RF port.	45
Figure 36: Block Diagram of the MMIC Mixer section.....	46
Figure 37: Block diagram of the solid-state power amplifier section.	48
Figure 38: Measurement setup diagram of the intermediate frequency section.....	49
Figure 39: Test Jig used for measurement of the intermediate frequency section.	49
Figure 40: Measured input return loss of the intermediate frequency section (10 dB per division scale).....	50
Figure 41: Measured output return loss of the intermediate frequency section (10 dB per division scale).....	51
Figure 42: Measured intermediate frequency section transfer function S21 as a function of frequency (10 dB per division scale).	52
Figure 43: Measured intermediate frequency section transfer function S21 as a function of frequency, with 1 dB per division scale.	53
Figure 44: Test jig used for measurement of the mixer section.	53
Figure 45: Measurement setup diagram of the mixer section	54
Figure 46: Measured mixer RF port power spectrum as a function of frequency.	54
Figure 47: Measured mixer RF output power variation as a function of frequency (1 dB per division scale).....	55

Figure 48: Measurement setup diagram of the band-pass filter section.....	56
Figure 49: Measured filter input return loss as a function of frequency.	56
Figure 50: Measured filter transfer function S21 as a function of frequency.....	57
Figure 51: Measured power amplifier input and output return loss (S11 and S22), and forward (S21) and reverse (S12) transfer characteristics, as a function of frequency.	58
Figure 52: Measured input-versus-output power response, over temperature, for 29.75 GHz signal frequency.....	59
Figure 53: Picture of the Ka-band transmitter RF circuitry.	60
Figure 54: Automated measurement setup diagram of the transmitter unit.	60
Figure 55: Measured transmitter gain variation over frequency and temperature.	61
Figure 56: Measured transmitter input-versus-output power response at 50 °C ambient temperature.	62
Figure 57: Measured transmitter phase noise response as a function of the offset frequency from carrier.....	63
Figure 58: Measured transmitter output power spectrum as a function of frequency at – 30 °C ambient temperature.	64
Figure 59: Return channel link between terminal located in Paris, France and hub located in Betzdorf, Luxemburg, over Ka-band satellite ASTRA 1H.	67

1 INTRODUCTION

Ka-band satellite networks have recently emerged to address a growing demand for high speed Internet access. These networks have the ability to deliver wide bandwidth (up to 38 Mbps in forward channel, and up to 2 Mbps in return channel) in a relatively inexpensive way since no costly infrastructure is required.

The main objectives of this project are:

1. To present a Ka-band Transmitter (part of satellite interactive terminal), used in a new generation of broadband, interactive networks for Internet protocol and multimedia content transfer over Ka-band geostationary satellites. The Ka-band transmitter is a part of the return channel link for data transport from customer site, over satellite, to the hub connected to Internet backbone.
2. To compare performance of this transmitter against requirements of the specifications outlined in the Digital Video Broadcast – Return Channel over Satellite standard document ETSI EN 301 459 [1].
3. To evaluate how a network employing a SIT with the transmitter in question, performs from system perspective, in particular, examining the availability of the service given a specific transmit data rate.

To this end, Section 2 provides background material on Internet applications and their performance over long latency networks, reviews current satellite networks with special focus on the ASTRA Ka-band Broadband Interactive network. Section 3 presents the satellite interactive terminal, with particular focus on the outdoor unit and transmitter. Design considerations and simulation results of the transmitter upconverter section are outlined in Section 3.3. Measurement results, at the sub-circuit level and unit level, are given in Section 3.4. The return channel link budget analysis is illustrated in Section 4.

The results can be summarized as follows:

1. Sub-circuits measurement results are very close to the simulated.
2. The unit results exceed the required specification with a considerable margin.
3. Link budget calculations show that an availability of service equal to 99.7%, with a data rate of 348 Kbps, can be achieved if the presented transmitter/outdoor unit is deployed in the ASTRA broadband interactive satellite network.

2 BACKGROUND

This section presents a quick historical review of the Internet, and outlines Internet applications and their performance over long latency networks. Secondly, current and emerging Ka-band satellite networks are described.

2.1 Internet Over Satellite

The Internet is a group of computer networks, each containing multiple sub-networks and computers that are organized in a tiered hierarchy. As a growing number of people are connecting to this vast information pool, providing new, high-speed data access methods is imperative.

Internet service providers have customers worldwide. Corporations are interconnecting geographically dispersed server networks. Universities are communicating across countries, sharing research information and their libraries.

Geostationary Earth orbit (GEO) satellite networks are ideal for interconnecting these widely dispersed servers, many of them in isolated geographical areas (islands) and or in places where cable infrastructure does not exist.

2.1.1 Historical Review

In the 1960s the US Defense Advanced Research Project Agency (DARPA) started research on linking computers in networks. Bolt, Beranek and Newman (BBN) were assigned the task of designing a communication protocol. The original network connected four sites in California and was the first to use Network Control Protocol (NCP), the first packet switching scheme for transferring data between computers.

In 1983, DARPA adopted TCP/IP (Transmission Control Protocol/Internet Protocol), which provided the robust protocol needed to support information transfer between different networks with different types of media. TCP/IP is still in use today.

In 1983 the network was split into two networks, Milnet and ARPANET. At the same time several other networks, like CSNET (Computer and Science Network) and BITNET, became a part of this growing network.

In 1987 the National Science Foundation (NSF) creates a high-speed backbone network connecting several super computer centers across the US. System also includes a number of mid level networks that provide access to a high-speed backbone

network. This backbone network is served by a non-profit organization, Advanced Networks and Services (ANS). At the same time profit companies began to develop the regional networks that provided access to backbone Internet and started carrying commercial traffic as well as NSF traffic. As a result, NSF established an "appropriate use policy", which limited the traffic through their backbone to non-commercial traffic only. Because of that policy, a group of regional networks formed the Commercial Internet Exchange (CIX) system, to create connection between the regional networks without using the NSF backbone.

The traffic on the Internet today is primarily carried through the commercial network with links to the NSF network.

2.1.2 Internet Applications

TELNET was one of the first Internet applications. It provided users at remote locations the ability to log on to another computer (host) and interact with it just as he would by using terminal he was directly connected to.

FTP (File Transfer Protocol) was the second Internet application. It enabled users at remote locations to search directories of any host computer on the Internet and transfer desired files from the host computer to his remote computer.

SMTP (Simple Mail Transfer Protocol) was developed to manage the transfer of electronic mail messages from one location to another.

HTTP (Hypertext Transfer Protocol) establishes the rules for transmitting hypermedia documents electronically and is associated with the World Wide Web (WWW) traffic.

WWW is a cataloging tool, and is successor of Archie, Gopher and Veronica, whose user-friendly interface allowed non-technical people to use this valuable resource.

Newer Internet applications include email, video teleconferencing and broadcast.

They all use IP (Internet Protocol) as the transmission mechanism, so that they can effortlessly run over satellite networks. However, performance levels vary from application to application as their requirements for network bandwidth and delay and implementation techniques are different.

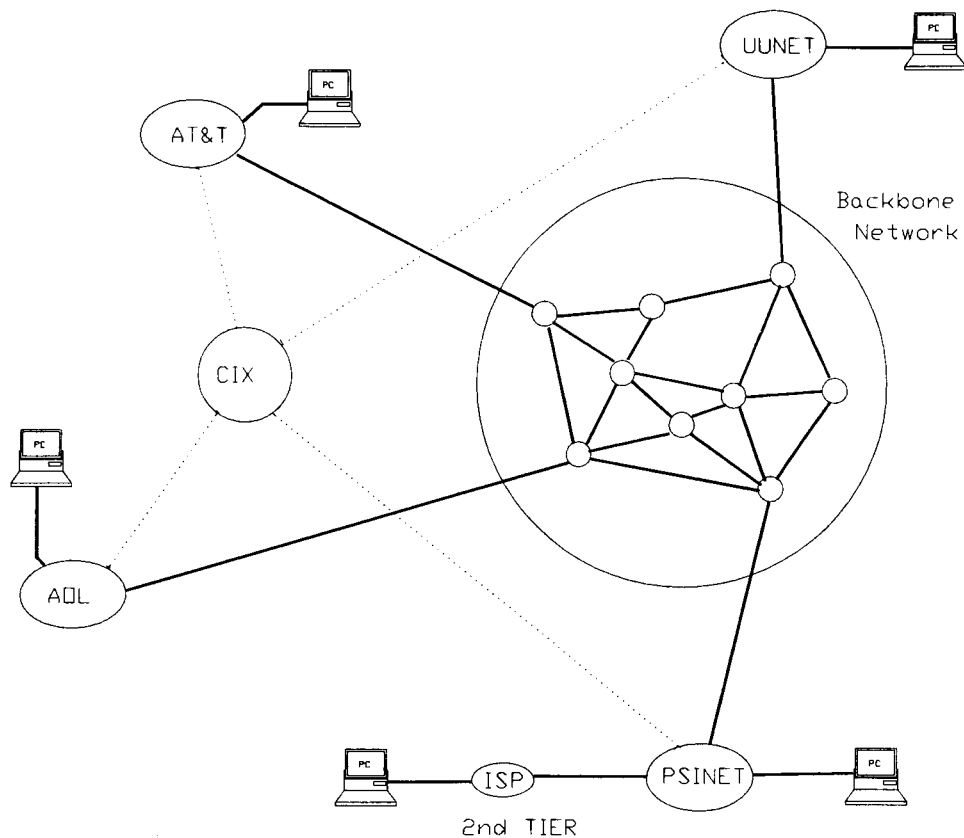


Figure 1: Internet network topology.

Data broadcast, such as webcasting, network news, TV and radio programs, is ideally suited for GEO satellites. Satellite networks can bypass tens of intermediate nodes, which significantly reduce the chances for packet drop and large delay jitter due to congestion. Compared to this, broadcast over terrestrial Internet can be very expensive.

Electronic mail is not interactive, so it can work over any network.

Videoconferencing and video distribution can be built on user datagram protocol (UDP). This protocol does not require bi-directional synchronization, so delays can be tolerated. Compared with terrestrial Internet, GEO satellites can provide better quality thanks to network simplicity and available bandwidth.

Remote control and login are delay sensitive, but if the user can accept a half-second to one-second delay, the application can run efficiently, as the response over GEO satellite is more stable.

Because data retrieval requires reliable transmission, many applications (such as WWW, FTP) use Transmission Control Protocol (TCP), which is sensitive to transmission delays, since "acknowledge-and-retransmit" method is used.

This limitation can be mitigated, with special processing techniques. Some of these techniques are presented in [2]. With special attention to design, the compensations can be made transparent to the end user application.

Table 1: Internet applications grouped by commonly used protocols.

GEO Satellite	
Internet Protocol (IP)	
TCP	UDP
Remote Login	Reliable Multicast
Electronic Mail	- Information Dissemination
	- Broadcast
On-line Information Retrieval	Real-time Protocols
	- Video Conferencing
	Gaming

2.2 Geostationary Satellite Networks

Current Internet backbones and sub-networks are mostly wired terrestrial networks, using cable, fiber optics and telephone lines. Bandwidth available in these networks ranges from 1.5 Mbps (T1) to 622 Mbps (OC-12).

Among emerging mobile/wireless networks, GEO satellite networks present great potential with their ability to broadcast and multicast large amounts of data over a widespread area.

Geostationary Earth orbit (GEO) satellites have a circular orbit on a plane equivalent to Earth's equatorial plane, at synchronous altitude of 35,800 km. Since a satellite's orbital period is identical to the Earth's rotational period, the satellites appear stationary from the Earth's perspective.

Internet distribution over GEO satellite has following advantages:

- Relatively inexpensive because no costly infrastructure (cable-laying) is needed; one satellite covers a large area
- High bandwidth allows transfers at high rates
- In comparison with the terrestrial mesh interconnection network, GEO satellite networks have simpler path (fewer hops), which often results in better network performance.

As discussed in [2], the major challenge that GEO satellite networks present to the performance of Internet applications is the communication delay (latency) between two Earth stations connected by satellite. The delay ranges from 250 ms to 400ms (including on-satellite processing). This delay is 10 times higher than a multi-hop, fiber optics path across North America, and may affect interactive applications (like TCP) that require synchronization (handshaking) between two sites.

Use of low Earth orbit (LEO) and medium Earth orbit (MEO) satellites can circumvent this problem, because their communication delays are just two times higher than those with terrestrial fiber optics connections. Because of the nature of their orbits, a constellation of satellites is required to provide a full coverage. The analysis presented in [3] shows that the result is complex network management at greater cost. The initial investment required for a LEO or MEO satellite network is well above \$1 billion, whereas the GEO's is below \$200 million. In addition, Earth terminals will be impacted, because

the use of phased array antennas (tracking capability) will be necessary. A phased array antenna is significantly more expensive option than the classic offset parabola dish.

2.2.1 Review of Current Geostationary Satellite Networks

2.2.1.1 Dedicated Single Channel per Carrier Satellite Network Description

This type of network has dedicated point-to-point single channel per carrier (SCPC) links over satellite, to connect local point of presence (POP) servers to Internet gateway points.

Figure 2 shows a typical SCPC network topology.

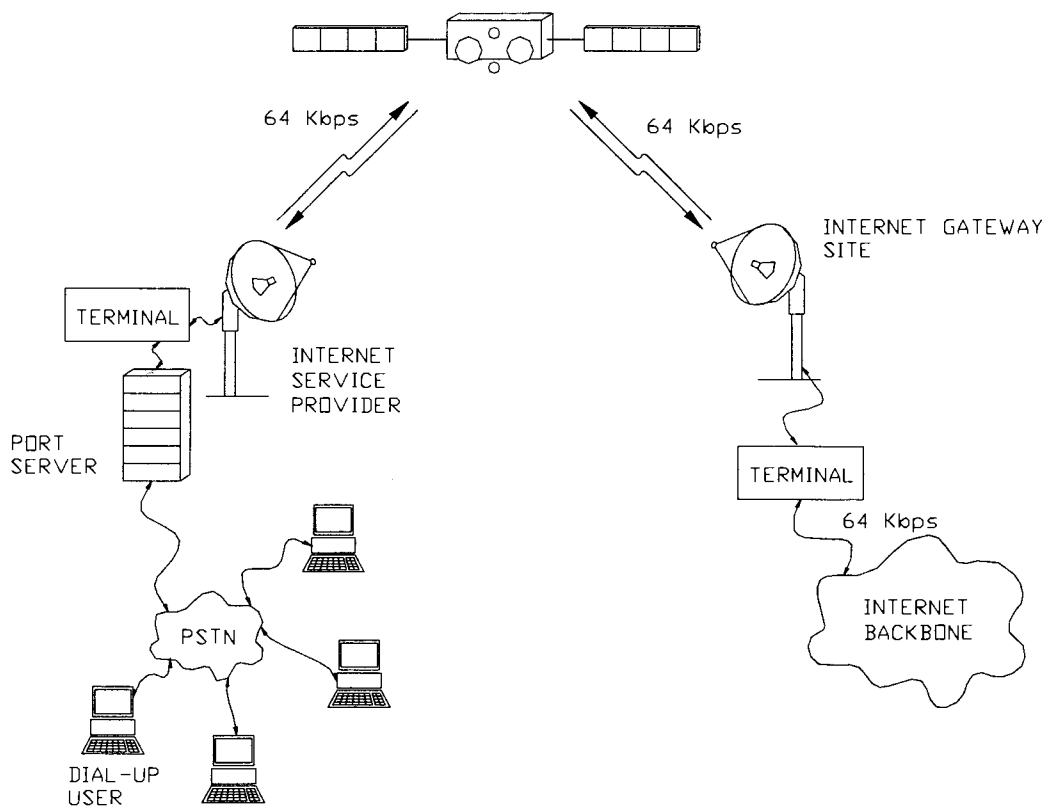


Figure 2: Dedicated single channel per carrier satellite network topology.

The satellite link establishes a full-time data connection between the Internet backbone and the local access point, at speed from 64 to 256 Kbps.

Users may access a server over a local area network (LAN), or through dial-up telephone lines connected to the public switch telephone network (PSTN). At any time there may be several simultaneous IP sessions. The routers located at either end provide session management.

As discussed in [4], constraints of this type of network are:

- Web browsing traffic and multimedia server transactions are more intensive from the server to the end user than in the opposite direction (10:1). These symmetrical satellite links are not needed since asymmetrical links are more efficient.
- In systems where traffic load varies widely, use of full-time fixed circuits is not economical because service provider's operating cost is high.
- For networks where there are multiple service sites, the use of dedicated links from the gateway to POP is inefficient and costly because of the need for dedicated hardware, associated overhead, etc.

In conclusion, implementation of some kind of resource sharing can be very cost effective and will provide improved service and performance.

2.2.1.2 Very Small Aperture Terminal Satellite Network Description

Traditional very small aperture terminal (VSAT) network, providing a service to variety of different sites, is shown at Figure 3.

Different sites shown are:

- Single client site, where the user is connected directly to a terminal
- Corporate access site, where the users are connected through a local area network, and
- Internet service provider site with wired dial-up access through a public switch telephone network.

For traffic from a gateway, time division multiplex (TDM) is used for capacity sharing. A single 256 or 512 Kbps data link is time shared among a large number of users. For each IP session the system allocates a portion of the total bandwidth, usually 16 to 32 Kbps.

Figure 3 illustrates VSAT network topology.

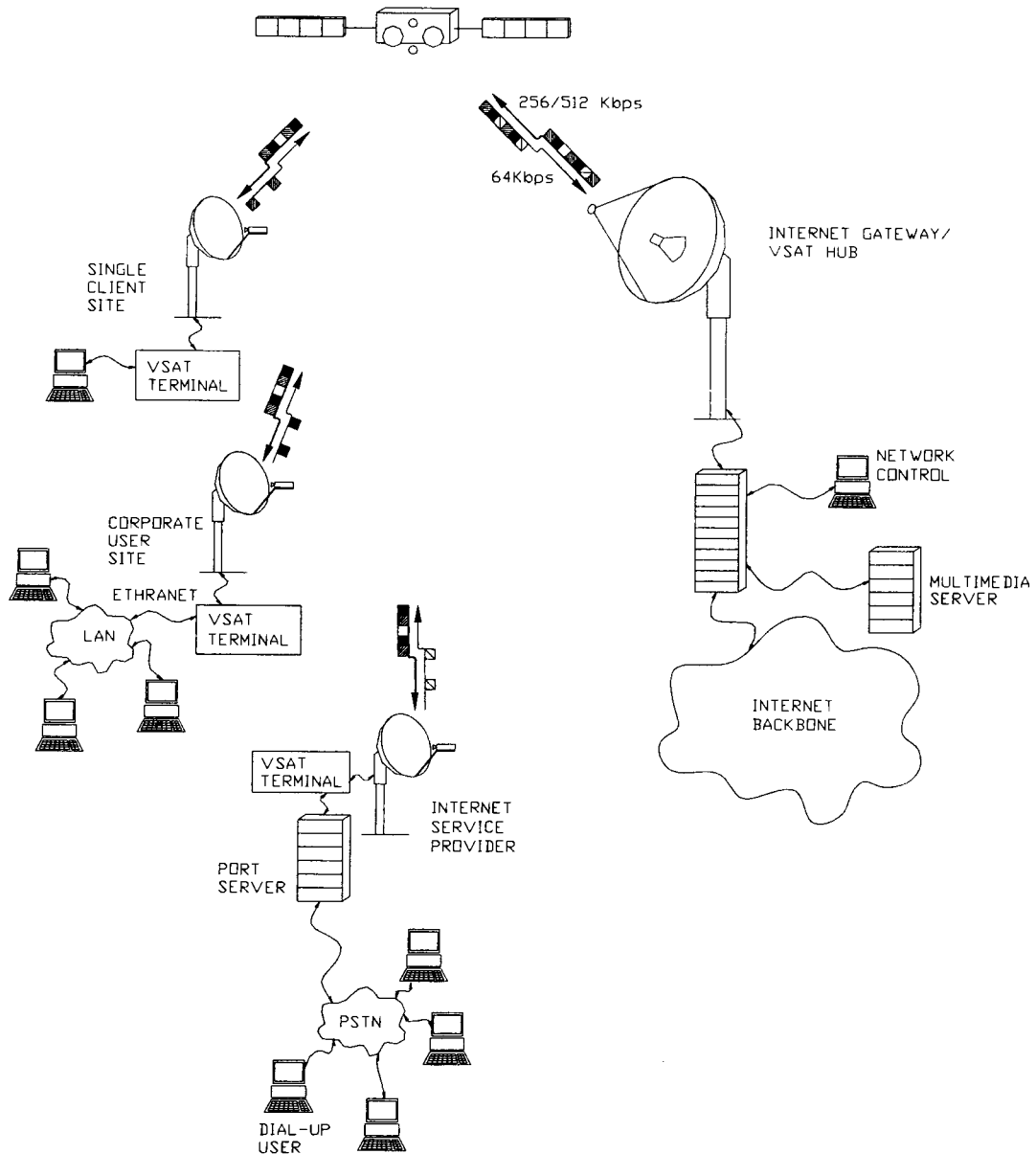


Figure 3: Very small aperture terminal satellite network topology.

For the traffic from terminals to the gateway, the time division multiple access (TDMA) technique is used. A single RF channel, with capacity of 64 Kbps, is time shared among sites.

Special protocols, in addition to TCP/IP protocol, are used to support this resource sharing technique.

TDM/TDMA VSAT systems are example of star network configuration, where all traffic passes through central hub (gateway). This traffic pattern may be acceptable for a single gateway, but for services that have many multimedia server locations, this is not the best solution.

VSAT systems were designed to be effective in transporting a small amount of data, associated with services like automated teller machines, credit card validation, point-of-sale and inventory. As a result, high bandwidth and more constant connections, needed for Internet and multimedia users, are not well matched for VSAT systems. Although they can provide a reasonable level of service, they are not cost effective solution.

2.2.1.3 Demand Assigned Multiple Access Satellite Network

Single channel per carrier (SCPC) demand assigned multiple access (DAMA) network is actually a hybrid between the SCPC point-to-point system and VSAT system. SCPC DAMA system is an example of a mesh network configuration - resources are allocated on user demand by connecting any two sites in the network using single carrier per channel link. This connection can be a full-duplex equal rate, unbalanced rate, one-way broadcast or multicast.

The control organization of the SCPC DAMA network is similar to the VSAT system in the sense that the resources allocation, type of connection and the administration are provided by a central controller, using TDM/TDMA VSAT communication at 19.2 Kbps rates.

Figure 4 shows a multi-gateway and multi-server network for Internet and multimedia data transfer.

The traffic from the gateway uses wide-band, one-way channel (256 to 2,048 Kbps), which is shared among all Internet user sites, with individual sessions having access to the full-bandwidth. If greater capacity is required, multiple 2 Mbps carriers can originate from the gateway. The users are charged for the quantity of data transferred.

Figure 4 presents SCPC DAMA network topology.

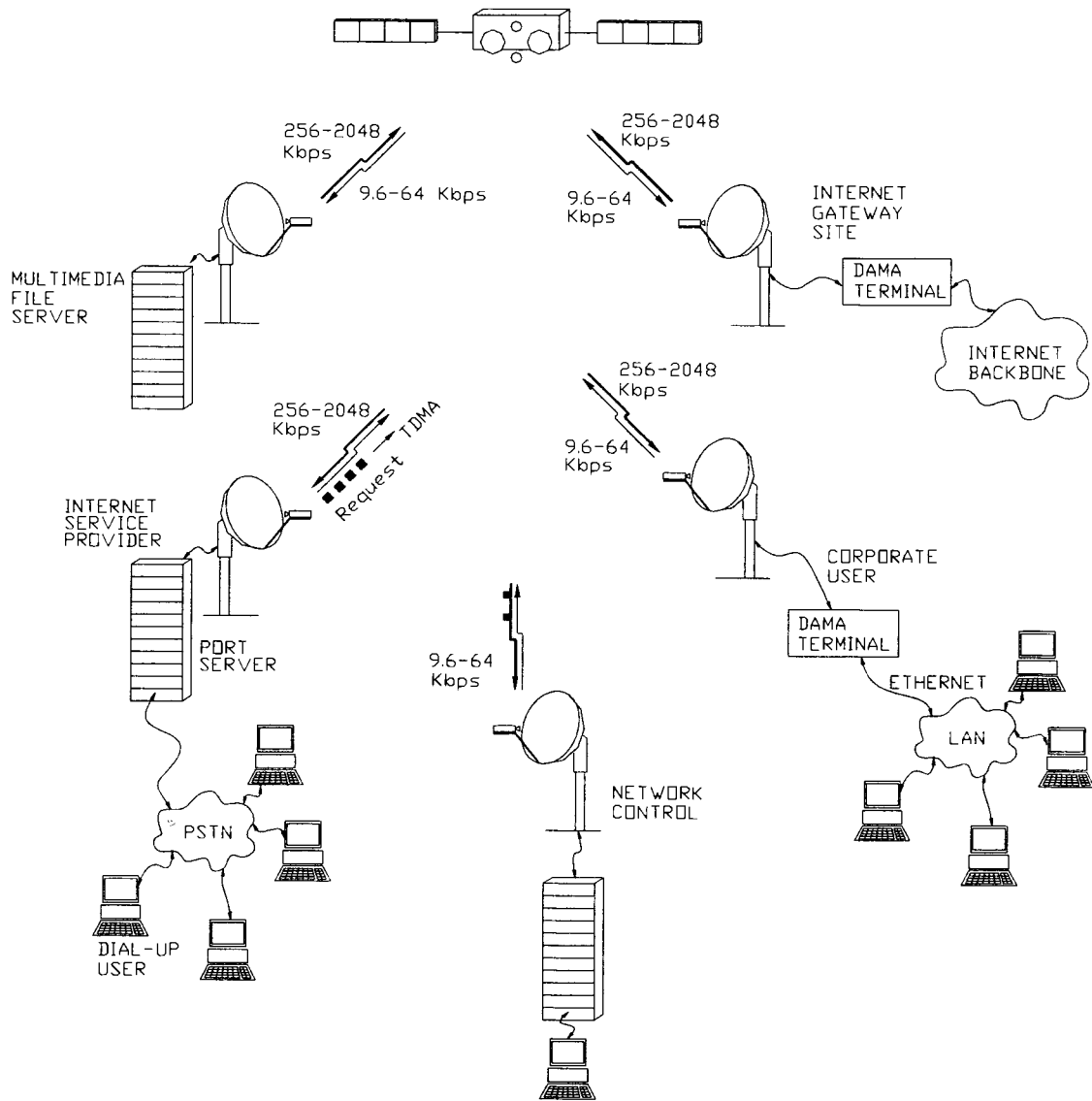


Figure 4: Demand assigned multiple access satellite network topology.

A return link established from each remote site to gateway uses data rates from 9.6 to 64 Kbps, depending on the traffic load at the user site.

All other systems are usually variations of the ones described above, either in a star, mesh or hybrid configuration.

2.2.2 Ka-band Satellite Networks

The Ka-band multimedia satellites are a new generation of satellites. As discussed in [3], they use on-board processing and switching as well as multiple pencil-like spot beams, to provide full two-way services, to and from small satellite interactive terminals (SIT's), located at the customer's premises. The SITs use antennas comparable in size with the current direct broadcast dishes. These satellites are also equipped with inter-satellite links operating at V-band (60 GHz).

The main advantage of multiple spot beams, each covering only a small area of the Earth, is frequency re-use, similar to a cellular phone network re-using a spectrum.

The SITs request bandwidth only when there is data to be sent ("bit rate on demand"), so that users pay only for the time that they use the link. This provides a flexible and cost effective solution, in contrast with conventional satellites where users usually pay for permanent leases.

Ka-band is subject to substantial interference from rain, which was a concern. NASA launched a Ka-band satellite in 1993, that uses all of the key technologies required for new commercial Ka-band satellites. The tests performed were successful, which allowed for further developments to proceed.

It was initially expected that 2.5 –3.5 GHz would be available for GSO satellites, but this was reduced by demands from non-geostationary satellites (LEO and MEO), Local Multipoint Distribution Systems (LMDS) and Mobile Satellite Service (MSS) links.

In addition, high-speed internet delivery systems that are competing with Ka-band satellite systems, like high-speed digital cable networks, asymmetric differential subscriber line (ADSL) and LMDS, are entering the marketplace.

Apart from high speed Internet access, a series of applications like videoconferencing and video telephony, data broadcasting, tele-medicine, tele-education, local television, news on demand and multimedia for businesses and personal use, are expected to develop as a result of this satellite technology.

This will have an interesting impact on the fast growing European market, discussed in the next section.

2.2.2.1 Ka-band Satellites

SES ASTRA is the first European satellite operator to commercially use Ka-band frequencies for interactive broadband services, over ASTRA 1H satellite at orbital position 19.2° East. In Q4 2000, SES commenced commercial Beta trials of the Broadband Interactive (BBI) system, for two-way asymmetric broadband collection and delivery of multimedia. ASTRA 1K, scheduled for launch in 2002, will add another 52 Ku and 2 Ka transponders, will provide full back-up for ASTRA 1H return path, and will extend geographical coverage (reference [5]).

Eutelsat Hot Bird 6 (HB6) satellite, will be located at orbital position 13° East, and will carry total of 32 channels, including 4 at Ka-band frequencies for internet and multimedia services. The satellite launch is scheduled for 2nd quarter of 2002. See reference [6] for details.

Figures 5 and 6 demonstrate the Ka-band uplink and downlink coverage. HB6 uses 4 spot beams for uplink coverage.

Alenia Spazio EuroSkyWay satellite will be located at orbital position 16.4° East. Scheduled for launch in 2003, this satellite will cover Europe and the Mediterranean Basin (see reference [7]). The satellite will have on board processing (OBP), and will provide bi-directional bandwidth on demand, dynamic resources allocation and pay per use.

HB6™ Ka-band uplink

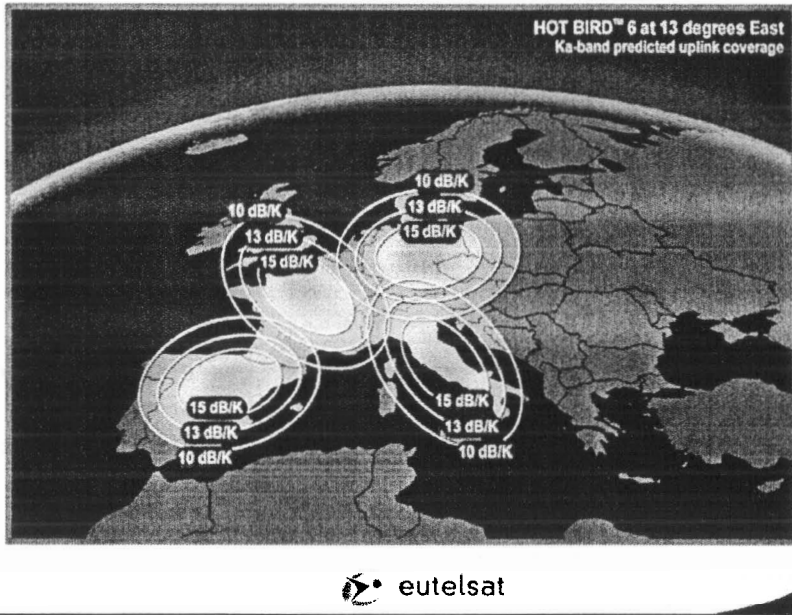


Figure 5: Hot Bird 6 satellite Ka-band uplink coverage.

HB6™ Ka-band downlink

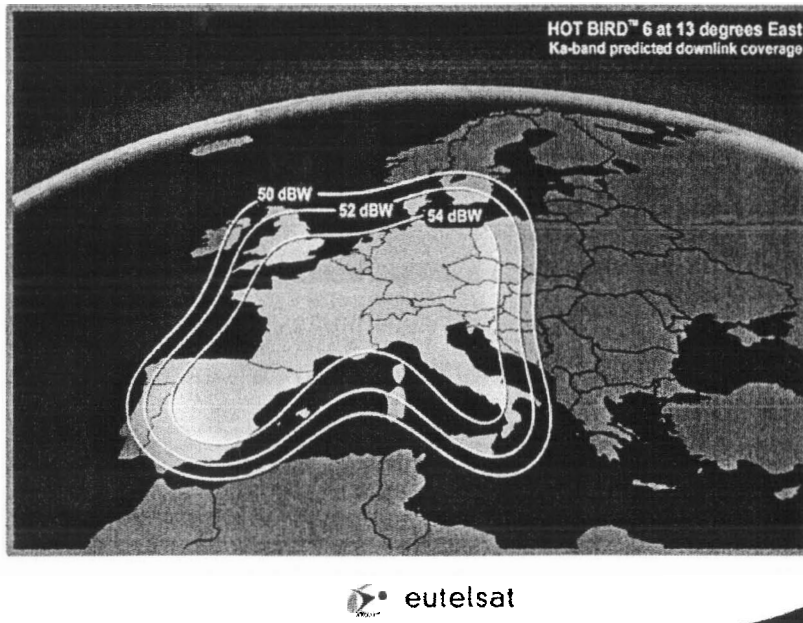


Figure 6: Hot Bird 6 satellite Ka-band downlink coverage.

2.2.2.2 ASTRA Broadband Interactive Network Overview

The ASTRA broadband interactive (BBI) network is a 2-way satellite-based broadband platform, specifically designed to provide Internet access and distribution of multimedia rich files. BBI is the first commercial implementation of the Digital Video Broadcast – Return Channel over Satellite (DVB-RCS) open standard.

The BBI system is an example of the star network configuration, where all traffic passes through a central hub (gateway).

This network supports all standard IP-based needs, such as file transfers, e-mail, database access and Internet access. The network contains:

- Single client sites, where the user is connected directly to terminal
- Corporate access site, where the users are connected through the local area network
- Internet service provider sites (cable operators and telcos) for easy extension of their terrestrial backbone to remote communities.

BBI can also support Tele-medicine and Tele-education services and monitoring of remote sites.

The Forward Path carries user traffic and signaling from the Hub to the SITs. Framing structure, channel coding and modulation is based on the standard digital video broadcast over satellite (DVB-S) transmission system.

The BBI Hub is capable of delivering up to 38 Mbps of IP data or multimedia content. The transmission is done at Ku frequency (10.7 to 12.75 GHz), over 120 channels, with 1dB bandwidth of 26 and 33 MHz. Orthogonal-linear polarization is applied. Odd numbered channels have nominally Horizontal polarization, while even numbered channels have nominally Vertical polarization.

The Return path carries user traffic and signaling from SITs to the Hub. The return path is based on a multi-frequency time division multiple access (MF-TDMA) scheme.

At the present time, fixed-slot MF-TDMA is in use, meaning that the bandwidth and duration of successive traffic slots used by return channel terminal is fixed. In the near future, dynamic-slot MF-TDMA will be deployed. When this occurs, return channel terminal may vary the bandwidth and duration of successive traffic slots, and may also change transmission rate and coding rate between successive bursts.

Figure 7 describes BBI network topology.

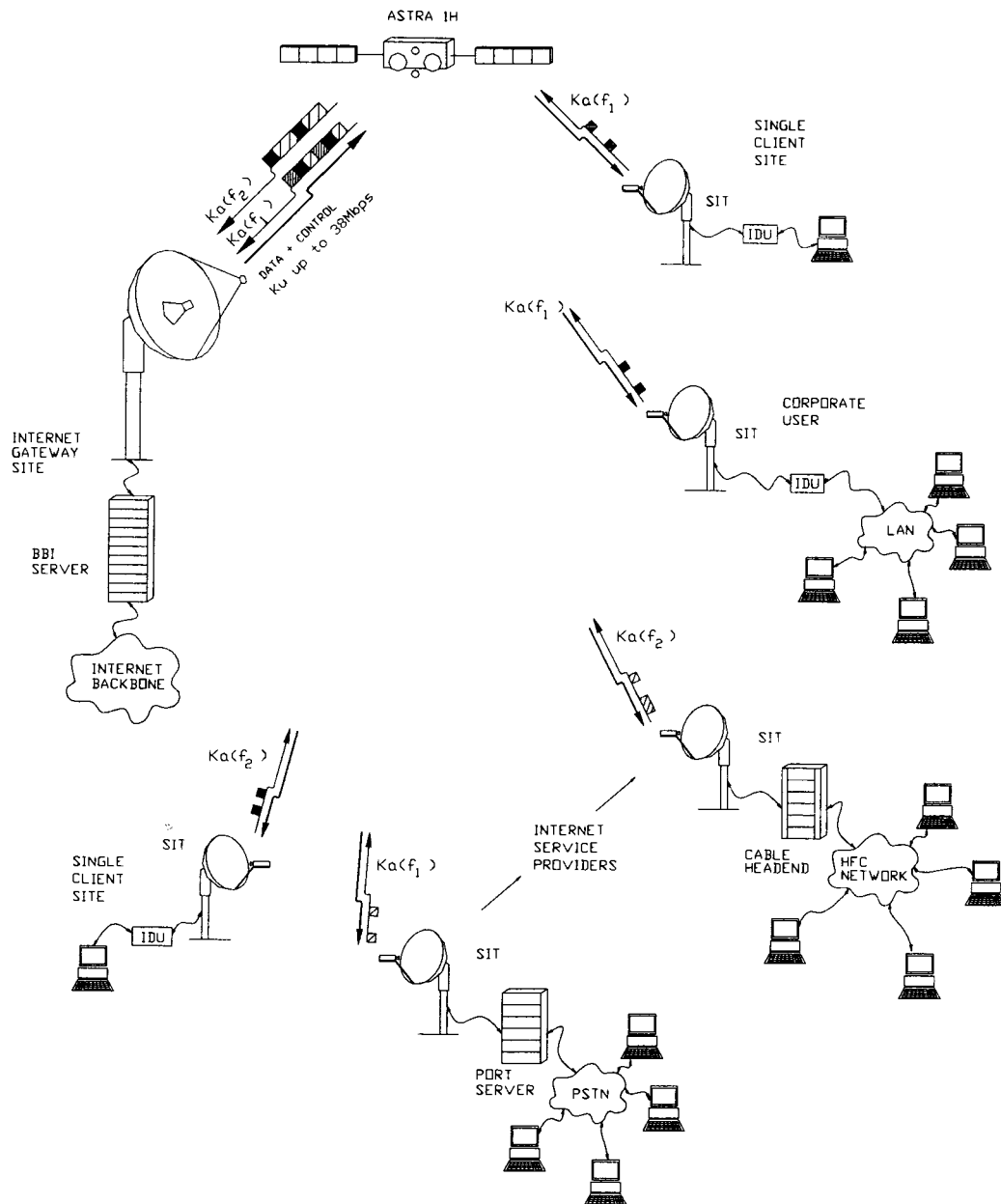


Figure 7: ASTRA broadband interactive network for IP transfer over Ka-band satellite.

The signal is modulated using conventional gray-coded quadrature phase shift keying (QPSK) modulation scheme, with baseband shaping performed using square root raised cosine filter with roll-off factor of 35%.

The return link transmission is done at Ka band (29.5 to 30 GHz), with data rates between 144 and 2,048 Kbps.

By combining polarization-division multiple access (PDMA) and space-division multiple access (SDMA), available frequency band is reused. The frequency band is divided into 8 orthogonal-linearly polarized channels (4 vertical and 4 horizontal). Each channel is received by satellite by separate receive spot beams. See figure 8 for details.

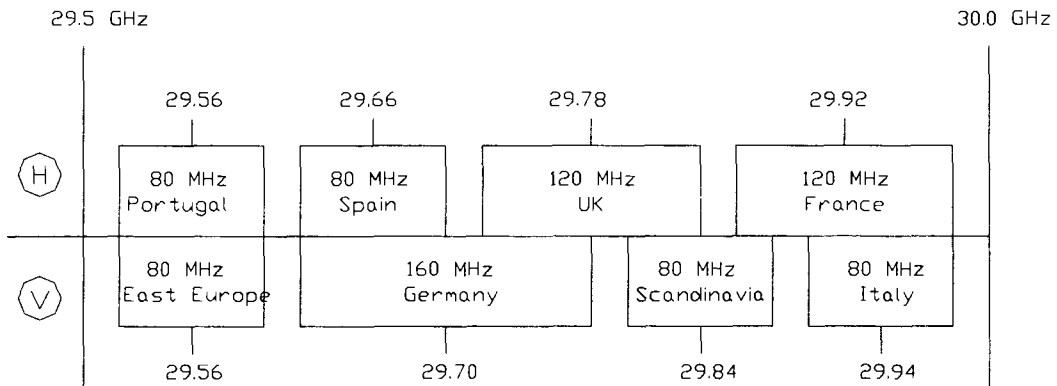


Figure 8: ASTRA network return link frequency plan.

The Air Interface of the BBI system is designed in accordance with the direct video broadcast return channel over satellite (DVB-RCS) system specification. This document has been published as a European Norm **EN 301 790** by the European Telecommunications Standards Institute (ETSI).

The receive characteristics of the SITs are contained in the ASTRA Reception Equipment Recommendations.

Table 2 shows comparison between different GEO satellite networks.

Table 2: Comparison table of geostationary satellite networks.

Ref.	Parameter	SCPC	VSAT	SCPC/ DAMA	BBI
1.	Network configuration	Point-to-Point	Star	Mesh	Star
2.	Modulation type used	QPSK	QPSK	QPSK	QPSK
3.	Forward Link Access Protocol	Dedicated link	TDM	TDM for control traffic	MPEG/DVB
4.	Return Link Access Protocol	Dedicated link	TDMA	TDMA for control traffic	MF-TDMA
5.	Forward Link Data Rates	64 – 256 Kbps	256 Kbps – 512 Kbps	256 – 2,048 Kbps	6 – 45 Mbps
6.	Return Link Data Rates	64 – 256 Kbps	64 Kbps	9.6 – 64 Kbps	144 – 2,048 Kbps
7.	Air Interface	Proprietary	Proprietary	Proprietary	Open standard

3 SATELLITE INTERACTIVE TERMINAL

This section outlines the Satellite Interactive Terminal (SIT), part of the Ka-band interactive network, with special attention to the outdoor unit and transmitter. Detailed design and simulation results of the transmitter's upconverter section are presented in Section 3.3. Measurement results are illustrated in Section 3.4.

3.1 General Description

The Satellite Interactive Terminal, illustrated in Figure 9, consists of:

- a fixed, small antenna with the transceiver – outdoor unit (ODU), located outside (roof) and pointed towards the satellite,
- an indoor unit (IDU), placed inside customer premises, and
- two-cable interfaculty link (IFL), connecting ODU and IDU together.

The IDU can be connected to a standalone multimedia PC or a local area network through 10BaseT Ethernet interface. ODU, on the other hand, receives and transmits data from/to satellite.

In the IDU, the data stream received from multimedia PC is encoded, modulated and translated to S-band (2.5 to 3 GHz) frequency. The S-band signal is then delivered to the ODU transmitter via IFL, where it is upconverted to Ka-band, and, using antenna interface, delivered to the satellite.

The SIT can transmit at data rates from 144 Kbps to 2,048 Kbps, depending on transmitter power levels and antenna sizes used.

The Ku-band signal from the satellite is received and down-converted by ODU, to L-band (950 to 2150 MHz) frequency. The L-band signal is then delivered to IDU via a second IFL cable, where it is demodulated to the base band (IF and baseband demodulators) data stream, decoded and delivered to a multimedia PC.

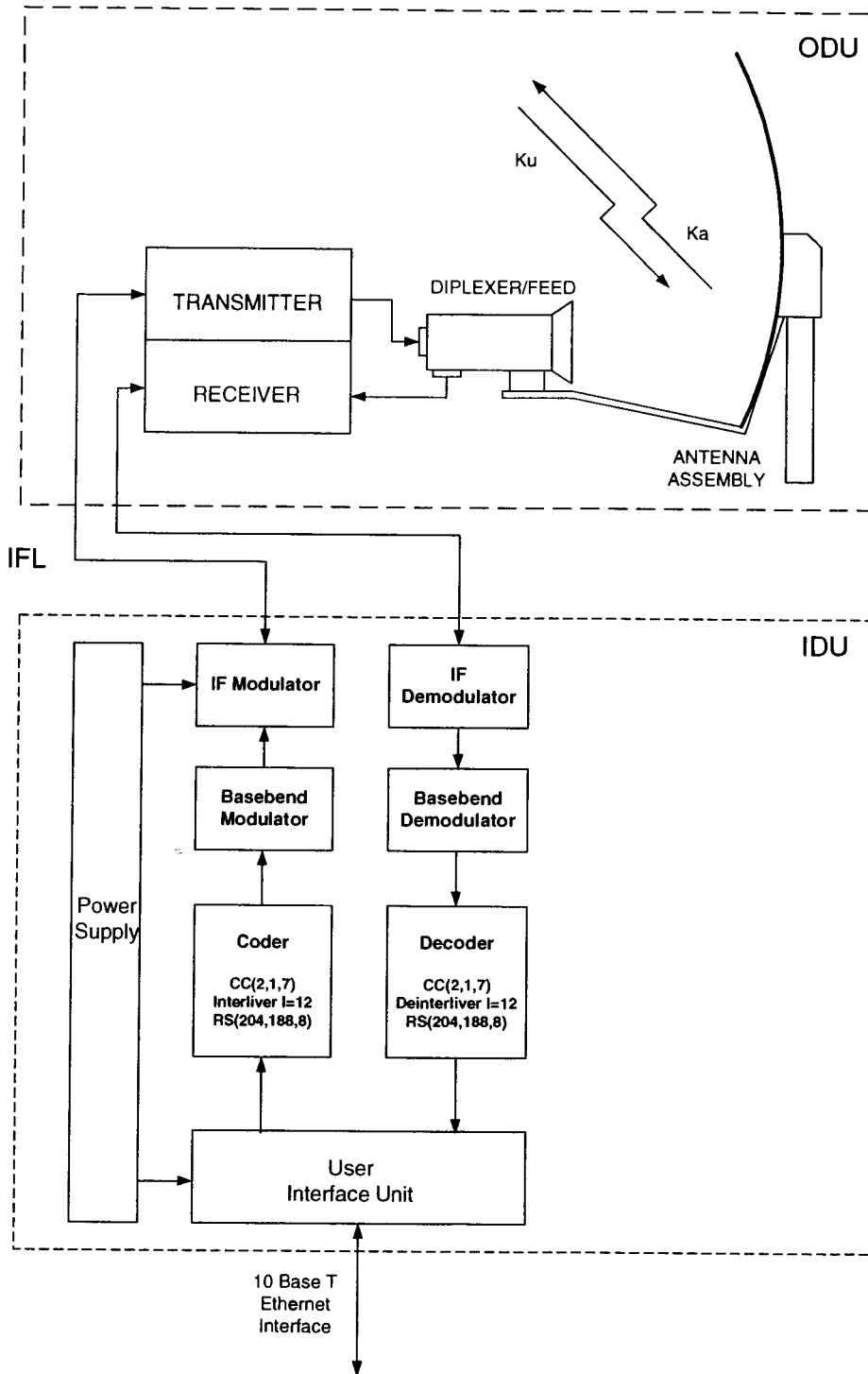


Figure 9: Block diagram of the satellite interactive terminal.

3.2 Outdoor Unit Overview

The outdoor unit (ODU), part of Ku/Ka-band satellite interactive terminal, as described by Fikart and Chan [8, 9], is composed of the following elements:

- Gregorian dual offset parabolic antenna with mount subsystem,
- 12/30 GHz dual feed/diplexer,
- Ku-band low noise block down-converter (LNB), and
- Ka-band transmitter

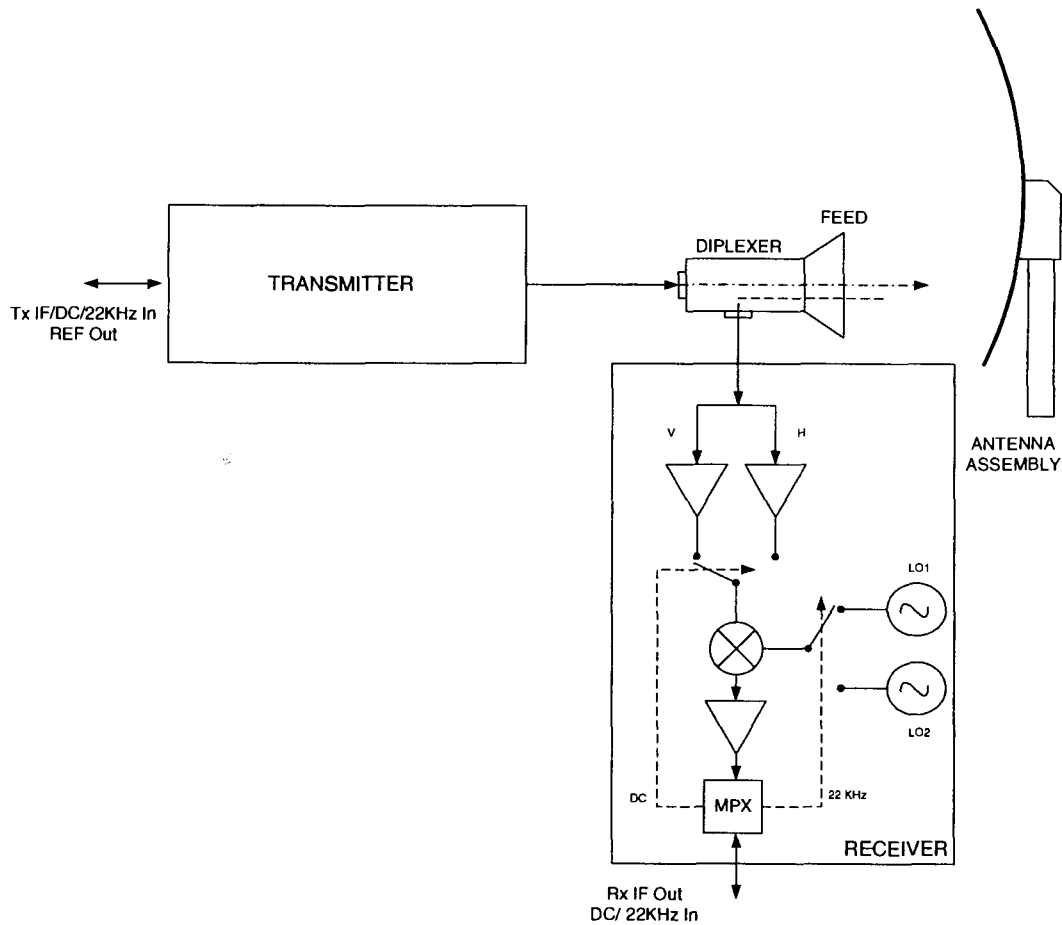


Figure 10: Block diagram of the outdoor unit.

The Ku-band LNB is attached to a diplexer via a C120 wave-guide flange. The Ka-band transmitter is mounted on the antenna boom, and attached to the diplexer via a flexible WR28 wave-guide.

The ODU is interconnected to IDU via an IFL, consisting of two coaxial cables.

Transmit IFL cable carries multiplexed:

- from IDU to transmitter: Tx IF signal, DC power and 22KHz Control and Monitoring signal,
- from transmitter to IDU: 10 MHz reference signal and 22 KHz Control and Monitoring signal.

Receive IFL cable carries multiplexed:

- from IDU to LNB: DC power and 22 KHz control (polarization/bend) signal
- from LNB to IDU: Rx IF signal

The Ku-band signal, received from the satellite by the antenna/feed system, is separated from transmit signal in the waveguide diplexer and delivered to the LNB. Two separate waveguide probes receive horizontally and vertically polarized signals, which are amplified with low-noise amplifiers (LNAs). One of the signals is selected (DC control received from IDU) and fed to the mixer for down-conversion. Ku low-band (10.7-11.7 GHz) is converted to the 950-1950 MHz, and Ku high-band (11.7 to 12.75 GHz) is converted to the 1100-2150 MHz band IF. Selection between low and high band is performed by a local oscillator (LO) signal selection (22 KHz control signal from the IDU). See Figure 10 for details.

The main ODU parameters are outlined in Table 3.

Table 3: Main parameters of the outdoor unit.

Ref.	Parameter	Specification
1.	Tx IF input frequency	2.5 – 3 GHz
2.	Tx RF output frequency	29.5 – 30 GHz
3.	Tx polarization	Linear, H or V, factory set
4.	Rx RF input frequency	10.7 – 12.75 GHz
5.	Rx IF output frequency	0.95 to 2.15 GHz
6.	Rx polarization	Linear, H or V controlled by IDU
7.	Minimum G/T	15 dB/°K
8.	Rx Noise Figure	1 dB max.
9.	LNB Gain	56 dB typical

Three different types of ODUs, with different Effective Isotropic Radiated Transmitted Power (EIRP) capabilities, are employed in the BBI network. These EIRP values must be achieved with adjacent channel spectral re-growth of less than -20 dBc.

The properties of different ODUs are outlined in Table 4.

Table 4: Properties of the different outdoor units.

Ref.	Parameter	ODU1	ODU2	ODU3
1.	EIRP	40 dBW	45 dBW	50 dBW
2.	Max. Antenna size	76 cm	90 cm	120 cm
3.	Antenna Gain	44 dBi	46 dBi	48 dBi
4.	Tx Power	26.5 dBm	29.5 dBm	32.5 dBm
5.	Max. data rate (Return Channel)	144 Kbps	384 Kbps	2048 Kbps

A picture of assembled Norsat ODU, with 76 cm antenna is presented in Figures 11 and 12.

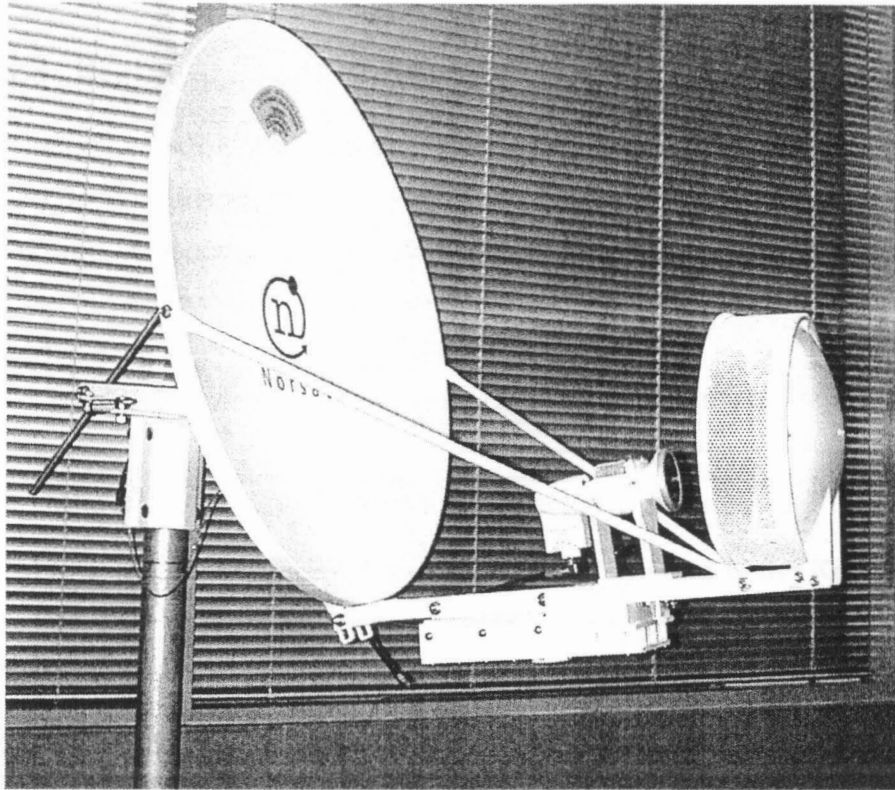


Figure 11: Norsat outdoor unit with 76 cm Gregorian dual offset parabola antenna system, transmitter and receiver with feed/diplexer.

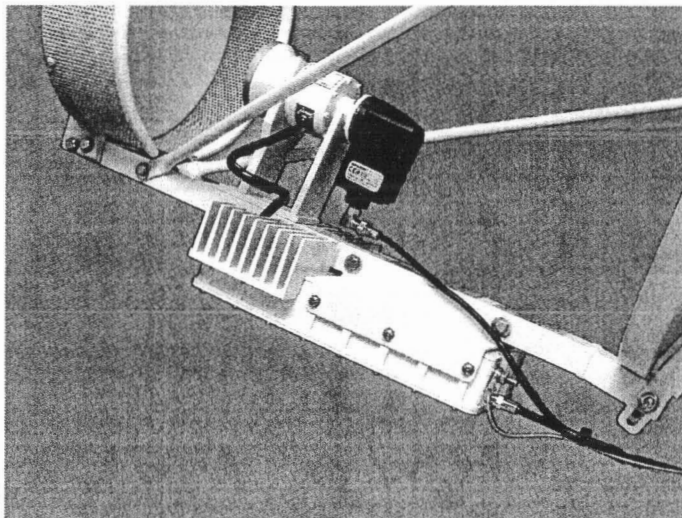


Figure 12: Norsat outdoor unit – boom arm assembly detail.

3.3 Ka-band Transmitter

Norsat NI-25512-01 Ka-band transmitter, part of the outdoor unit, designed for the ASTRA Broadband Interactive Network, enables return channel over satellite (RCS) IP transfer. Depending on the transmitter output power and antenna size used, data rates from 144 Kbps to 2048 Kbps can be transferred from the customer site, over satellite, to a gateway/hub.

The transmitter is designed to be compliant with ETSI EN 301 459 standard.

Main transmitter parameters are presented in Table 5.

Table 5: Main electrical and mechanical parameters of the Ka-band transmitter.

Item #	Parameter	Specification
1.	Input frequency band	2.5 – 3 GHz
2.	Input Impedance	75 Ω
3.	Input Return Loss 2.5 to 3 GHz 10 MHz	≥ 12 dB ≥ 8 dB
4.	Maximum Input Power	-20 dBm
5.	Output Frequency Band	29.5-30 GHz
6.	Nominal Output Power (20 dBc side band re-growth)	≥ 31 dBm
7.	Gain at any condition (small signal)	52 dB to 63 dB
8.	Gain Variation over Temperature (at any constant frequency) over total operating temperature range	< 6 dB p-p

Item #	Parameter	Specification
9.	Gain Variation in band (at any constant temperature) In any 20 MHz Band In full 500 MHz Band	≤ 1.0 dB p-p ≤ 5.0 dB p-p
10.	Phase Noise @ 10Hz/100Hz/1kHz/10kHz/>100kHz	$\leq -32/-62/-72/-82/-92$ dBc/Hz
11.	In Band Noise Emissions SSPA ON	≤ -95 dBm/Hz
12.	Output Spurious Level In band IF ON In band IF OFF Out of band, up to 40 GHz	≥ 60 dBc below single CW carrier at nominal output power ≤ -40 dBm (measured with 100 KHz RBW) ≤ -31 dBm
13.	Reference Signal Frequency	10 MHz
14.	Reference Signal accuracy/stability	$\leq \pm 30$ ppm
15.	Reference Signal Level	-10 ± 2 dBm
16.	Alarm Processing	Output amplifier and 10 MHz reference signal muted in event of LO alarm
17.	DC Power	13-30 VDC / 2.3 A max
18.	Power Consumption	≤ 30 W
19.	Input Interface	4 hole flange mount "F" female connector
20.	Output Interface	WR-28 waveguide flange
21.	Size (envelope dimension)	301 x 184 x 96 mm
22.	Mass	3.6 Kg
23.	Operating Temperature	-30 to +50 °C

3.3.1 Block Diagram

The transmitter upconverts the S-band (2.5-3 GHz) signal received from the indoor unit, and delivers a Ka-band (29.5-30 GHz) signal to diplexer/feed/antenna sub-system. DC signal and 22 KHz pulse width modulated (PWM) control signal are de-multiplexed and delivered to DC-DC and Monitoring and Control (MAC) circuitries, respectively.

Figure 13 shows transmitter block diagram.

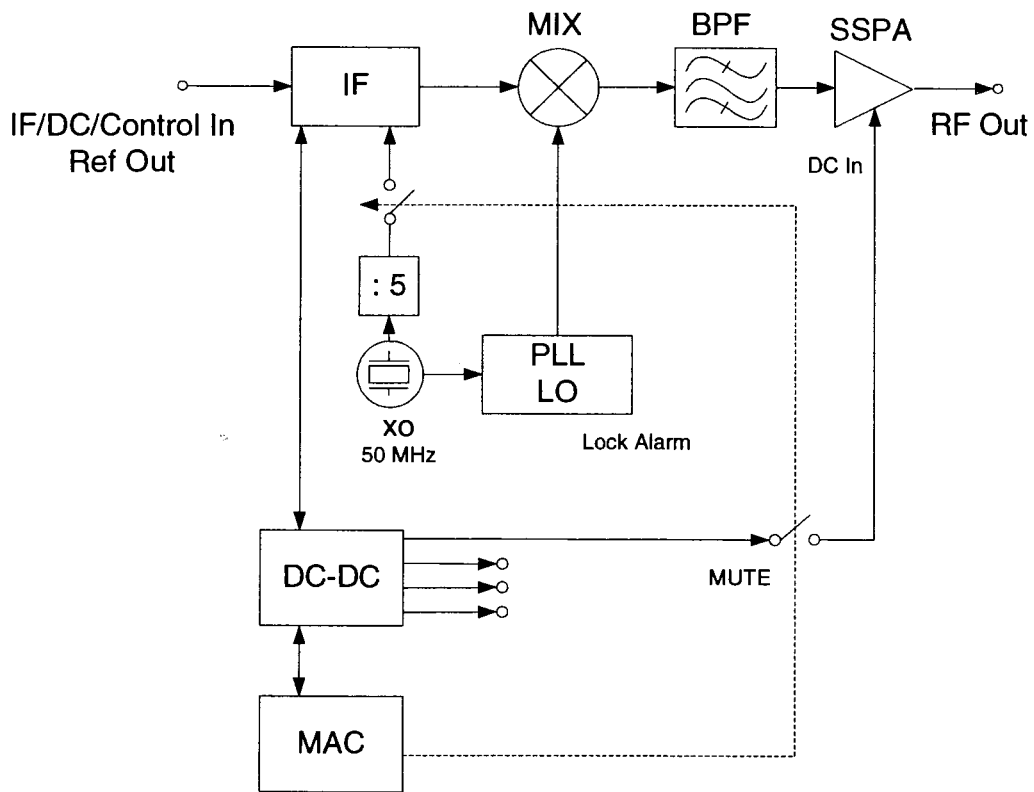


Figure 13: Simplified block diagram of the Ka-band transmitter.

Local oscillator (LO) circuitry generates a signal at 13.5 GHz, by doubling the 6.75 GHz signal from phase locked voltage controlled dielectric resonator oscillator (VCDRO). VCDRO is locked to internal 50 MHz reference using a sampling phase detector (SPD).

A 50 MHz modified Colpitts crystal oscillator is used to generate reference frequency for LO locking. The reference signal is also divided by 5, and sent back to IDU, via IFL cable. In the IDU, Tx 10 MHz reference signal is compared with the master reference received from the satellite, through a forward path. After error determination, the transmitter output frequency is corrected by adjusting the IF signal frequency.

The MAC circuitry is the monitoring and control module of the transmitter, and it uses a modified 22 KHz DiSeq protocol to act as a communication interface with IDU. Internally, in the case of the LO alarm (LO out of lock), the output amplifier section and 10 MHz reference signal output are muted immediately.

MAC circuitry provides following functions:

- LO Alarm (LO out of lock) monitoring
- Low voltage alarm (input DC voltage below 11 V) monitoring
- Output amplifier ON/OFF status monitoring
- Tx Enable/Disable command
- Remote software update

The transmitter can be enabled only when the appropriate password is entered.

The DC-DC circuitry converts incoming 13-30 VDC, into six different regulated voltages, required by other sub-circuits.

3.3.2 Up-converter Circuitry Description

A detailed description, containing block diagram, schematics and design considerations, of IF, MIX, BPF and SSPA stage is presented in this section.

This unit is standard a single conversion, no spectral inversion, block up-converter. The intermediate frequency (IF) signal received from IDU is processed in the IF section and then mixed with the local oscillator (LO), in the mixer section. The upper side band mixing product ($2LO + IF$), our desired signal, is then filtered and amplified.

Figure 14 illustrates spectral content at different points in the up-converter chain.

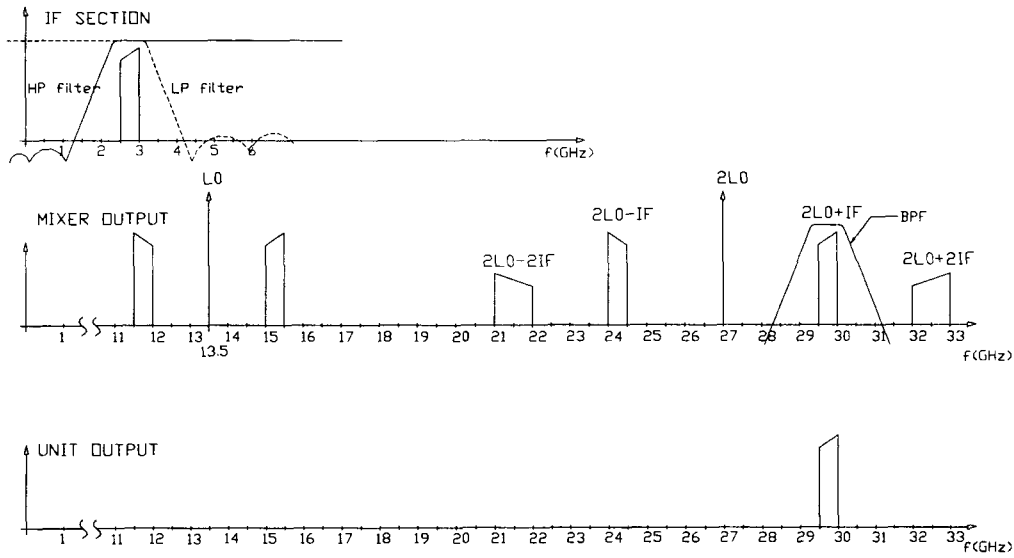


Figure 14: Frequency spectrum content presentation at the different points of the up-converter chain.

3.3.2.1 Intermediate Frequency Stage Description

The intermediate frequency (IF) stage de-multiplexes the S-band IF signal from DC, 22 KHz control signal and 10 MHz reference signal. The IF signal is filtered, equalized and amplified, and delivered to the Mixer section.

Figure 15 shows IF block diagram.

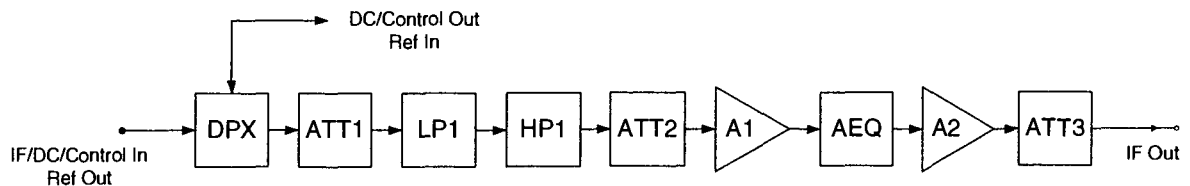


Figure 15: Block diagram of the intermediate frequency section.

3.3.2.1.1 Diplexer Section

The diplexer (DPX) is the first stage in the IF section chain, and its main task is to de-multiplex the IF signal from the other signals (DC, 22 KHz control and 10 MHz reference) with minimum insertion loss.

IF, DC and 22KHz control signals are received through a 75 Ω , F female connector (port P1 on schematic). A shortened, high impedance, $\lambda/4$ microstrip line (at 1.25 GHz), is used to split the IF frequency from other signals. For IF signal this line represents high impedance (parallel resonant circuit with resonance at 1.25 GHz), so the signal passes through the serial capacitor C2, to port P2 with minimum loss. At the same time, capacitors C1 and C2 present high impedance for all other signals (infinite for DC, $>1.5 \text{ M}\Omega$ for 22 KHz and $>3.39 \text{ K}\Omega$ for 10 MHz), so they are delivered to port P3 with minimum loss (10 MHz delivered from port P3 to port P1).

The diplexer schematic is shown in Figure 16.

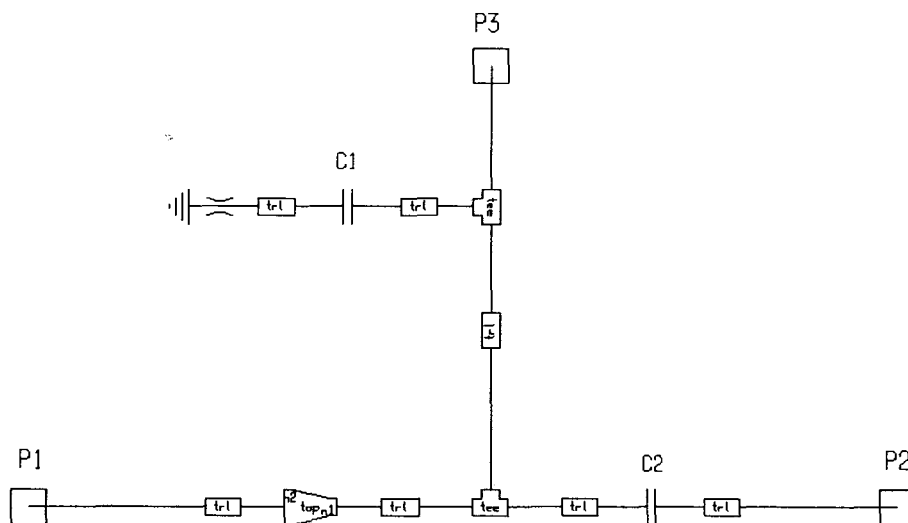


Figure 16: Schematic diagram of the diplexer stage.

3.3.2.1.2 Attenuator ATT1

The attenuator ATT1 is 2 dB, 75 Ω , T configuration attenuator, placed between diplexer circuitry and low-pass filter LP1 to improve matching.

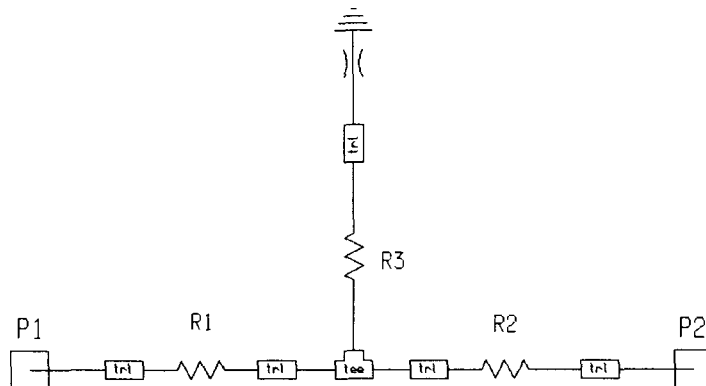


Figure 17: Schematic diagram of the attenuator ATT1.

3.3.2.1.3 Low-pass Filter LP1

The Low-pass filter LP1 is 9th order Elliptical, microstrip filter designed to transform input 75 Ω impedance to 50 Ω system impedance, and to prevent unwanted signals above 3.6 GHz to appear at the input of the first IF amplifier.

The Elliptical (also known as Caurer-Chebyshev) filter transfer function is characterized by equiripple response in the pass-band, and with the poles placed in such a way that minima of attenuation in the stop-band are identical (equiripple in the stop band). These filters are extensively discussed in literature. The catalog of normalized low-pass prototypes, with instructions for transformation to desired impedance and frequency is discussed by Zverev [10].

Modern simulation/synthesis CAD tools offer a much faster approach to the desired filter realization. In this case, the Ansoft [11] Serenade filter synthesis tool is used to generate lamped Elliptical filter with $f_{c3dB} = 3.2$ GHz, 0.4 dB insertion loss and 0.25 dBpp flatness in the pass band.

The filter schematic is shown in Figure 18.

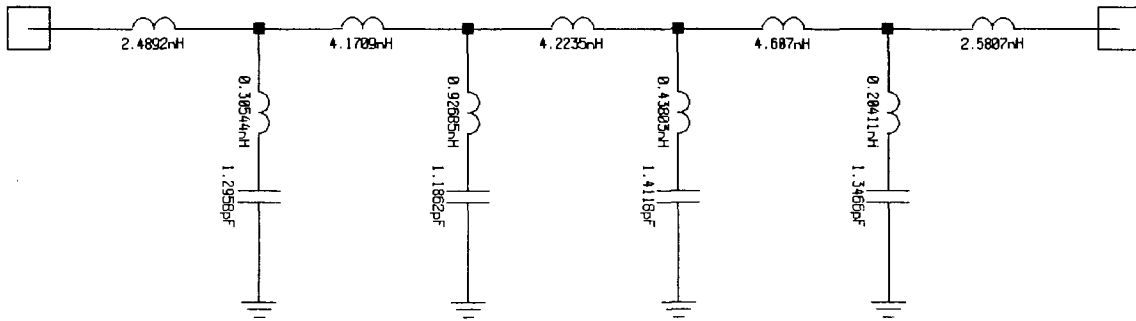


Figure 18: Schematic diagram of the low-pass filter LP1 with lumped elements.

Lumped elements are then substituted with microstrip distributed elements, and filter optimized using a simulation tool.

Series inductors are modeled as high impedance microstrip lines ($< \lambda/4$ long), while shunt series resonant circuits to ground, are replaced with shunt $\lambda/4$ microstrip open lines (at pole frequency). Step discontinuities (50 Ω to high impedance line interface) and T discontinuities (junction between two high impedance microstrip lines and shunt open stub) are taken into account by adding appropriate microstrip discontinuity models to simulation circuit (see Figure 19).

The ground plane is inserted between the shunt stubs, to decrease the amount of inter-coupling.

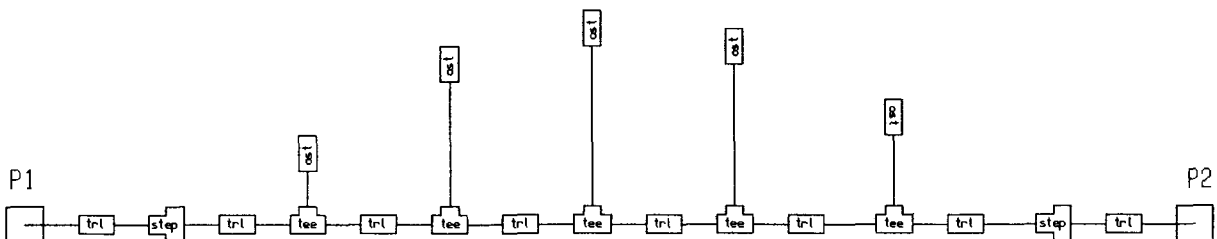


Figure 19: Schematic diagram of the low-pass filter LP1 with distributed elements.

Figure 20 shows the simulation results. Input/output return loss (S11 and S22) is $\leq -20\text{dB}$ in band, and transfer function S21 shows insertion loss of 0.6 dB at the band edge and in band flatness of 0.28 dBpp.

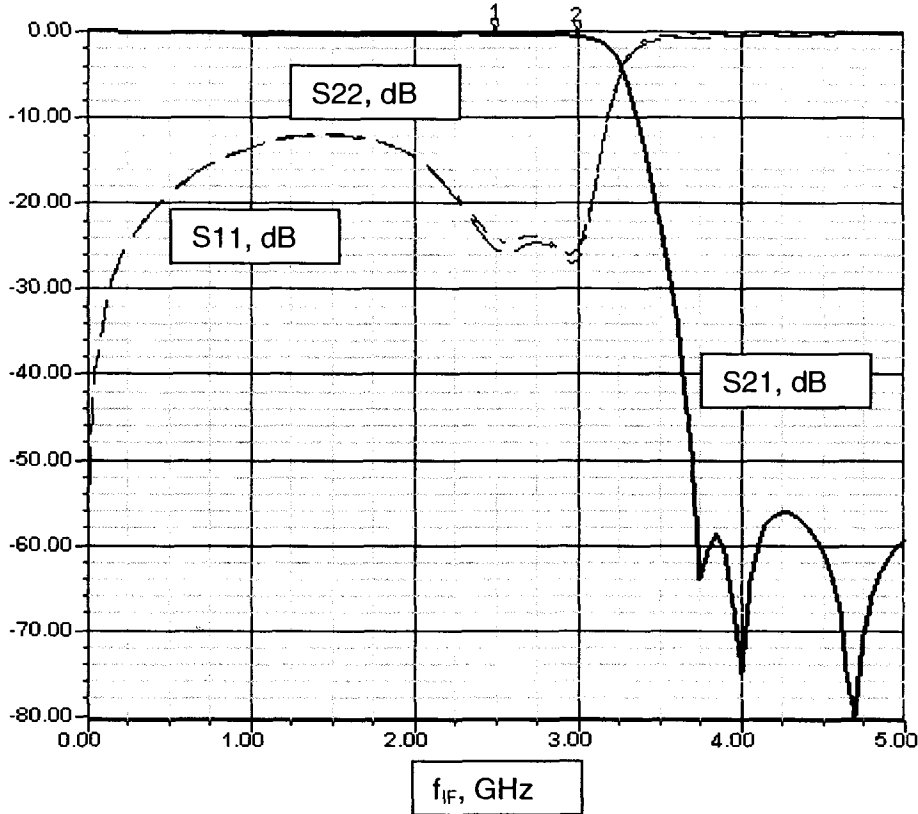


Figure 20: Simulated return loss and S21 transfer characteristics of the low-pass filter LP1.

3.3.2.1.4 High-pass Filter HP1

The high-pass filter HP1 is 7th order Elliptical microstrip filter; the next stage in the IF chain. The main task of this filter is to prevent unwanted signals below 2 GHz to appear at the first amplifier input, and cause in and out of band spurious signals upon mixing. 50-50 Ω , lumped Elliptical filter with $f_{c3dB} = 2.35$ GHz, insertion loss of 0.25 dB and 0.2 dB flatness is synthesized using Ansoft Serenade filter synthesis tool (see Figure 21).

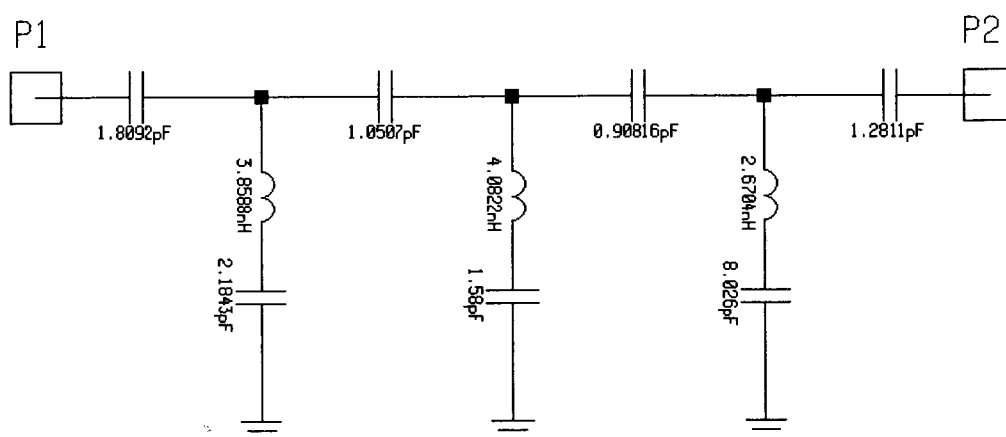


Figure 21: Schematic diagram of the high-pass filter HP1 with lumped elements.

Surface mount, lumped ceramic capacitors are used as series capacitances. Shunt series resonant circuits to ground are replaced with shunt $\lambda/4$ microstrip open lines (at pole frequency), except in a case of the last resonant circuit, which is replaced with high impedance microstrip line (inductance) followed by a lumped ceramic capacitor to ground. This approach is taken in attempt to decrease required board space.

This hybrid structure is then optimized using Ansoft Serenade simulation tool. As described in LP1, microstrip step and T discontinuities are taken into consideration by adding appropriate discontinuity models to simulation circuitry.

Figure 22 shows the HP1 filter simulation schematic. Filter simulation results are illustrated in Figure 23. Input/output return loss is ≤ -20 dB in band, and transfer function S21 shows insertion loss of 0.92 dB at the band edge and in band flatness of 0.35 dBpp.

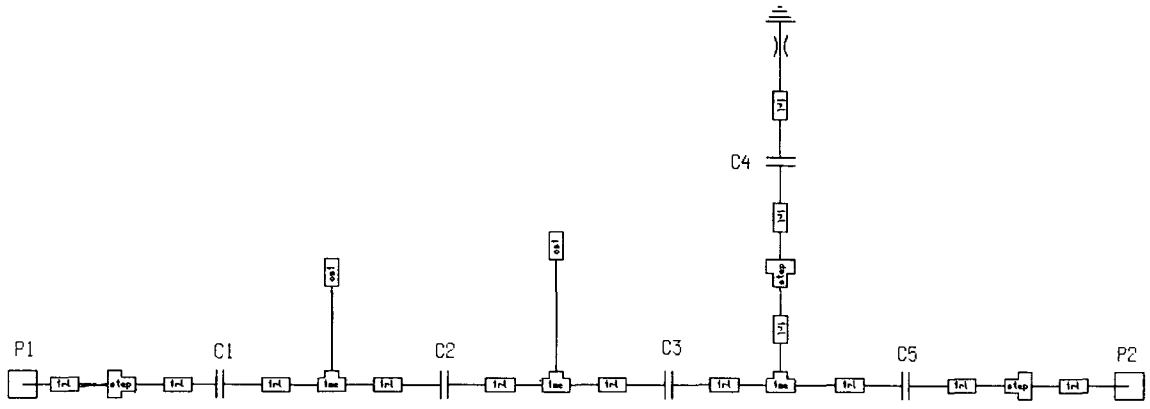


Figure 22: Schematic diagram of the high-pass filter with distributed elements.

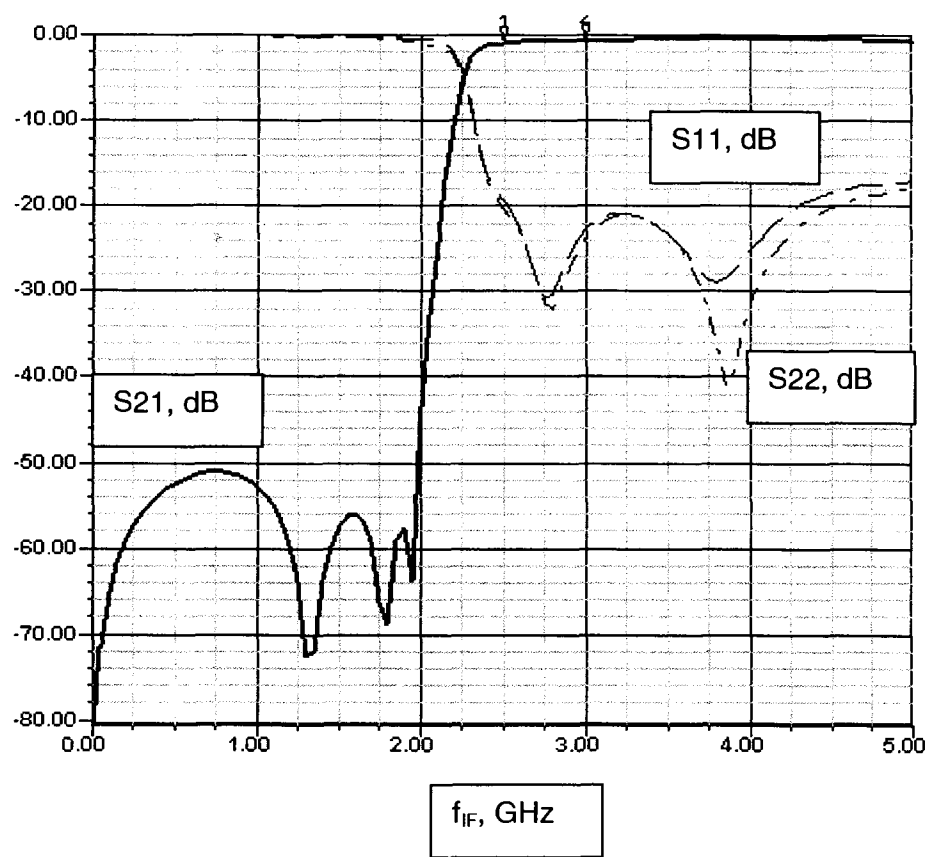


Figure 23: Simulated return loss and S21 transfer characteristics of the high-pass filter HP1.

3.3.2.1.5 Attenuator ATT2

Attenuator ATT2 is 2 dB, 50 Ω , T configuration attenuator placed between high-pass filter HP1 and amplifier A1 to improve matching. Schematic is similar to schematic diagram of the attenuator ATT1.

3.3.2.1.6 Amplifier A1

Sirenza Microdevices [12] SGA series, DC-3.2 GHz, Silicon Germanium Hetero-structure Bipolar Transistor (HBT) microwave monolithic integrated circuit (MMIC) is used as the first gain block. The SGA series uses a Darlington pair transistor configuration with properly chosen bias and feedback resistor. This specific amplifier is chosen since has good return loss, low noise figure ($NF \leq 4\text{dB}$) and output 3rd order Intercept Point (IP3) of $>27\text{dBm}$ (with 3.6V / 60 mA bias). Figure 24 shows schematic diagram of the MMIC amplifier with surrounding circuitry.

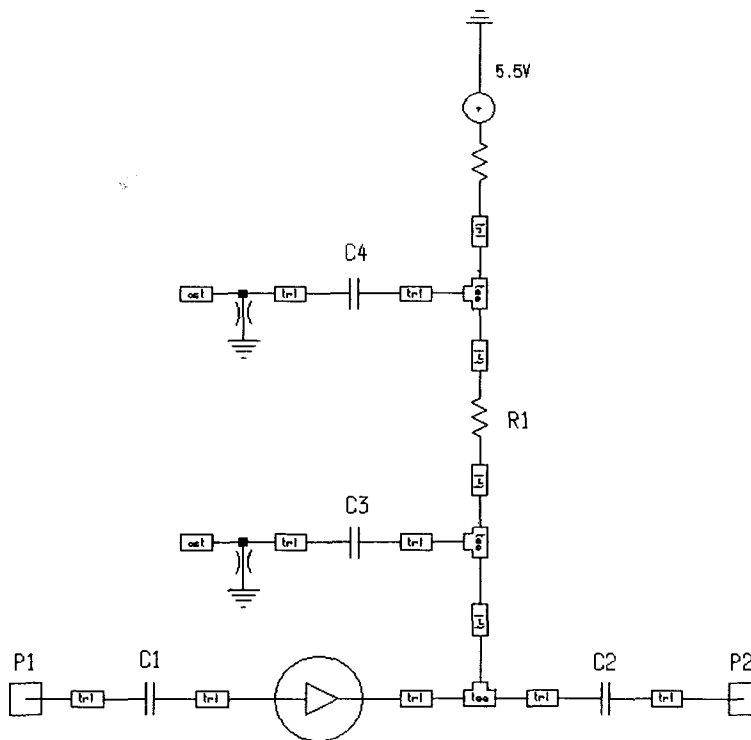


Figure 24: Schematic diagram of the MMIC amplifier A1 and biasing circuitry.

The output node of the MMIC is also used to provide bias voltage. In order to prevent loading of the output of the amplifier, the DC bias is fed to the amplifier through

a $\lambda/4$ (at 2.75 GHz), high characteristic impedance microstrip line, shorted with capacitor C3.

Looking from the amplifier perspective, this line has high input impedance (represents parallel resonant circuit, with resonance at the middle of the IF band), so IF power is delivered to port P2 with no loss at biasing point. Reactance of 10 times higher than system characteristic impedance (50Ω) is desired to prevent amplifier loading by the bias circuitry. Capacitor C3 self-resonance frequency is taken into consideration during capacitor selection ($f_{sr} > 4\text{GHz}$).

Since the output voltage is determined by design, the amplifier is biased using a current source. The simplest current source is a voltage source (V_{cc}) with resistor in series (R1). Resistor value is selected in such a way that required DC voltage (V_d) appears at the output with a desired I_{cc} current (3.6 V with 60 mA).

$$R1 = (V_{cc} - V_d)/I_{cc}$$

Power dissipation in the resistor R1 must also be considered during resistor package/size selection. The chosen package must have at least 40% higher power dissipation capabilities than the actual power dissipation.

It is important to maintain the desired bias current I_{cc} , since any changes in the current will change amplifier parameters such as $P1_{db}$ and $IP3$. Amplifier output DC voltage (V_d) varies with temperature with negative coefficient. Resistor R1 compensates that change since $I_{cc} = (V_{cc} - V_d)/R1$. Bigger resistor R1 provides more compensation, but at the same time higher supply voltage V_{cc} is required.

Two blocking capacitors, C1 and C2, are preventing DC loading of the amplifier by adjacent circuits.

Capacitor C4 with resistor R1 forms RC low-pass filter which function is to prevent low frequency components, like 300 KHz power supply switching signal, to reach amplifier and cause intermodulation spurious.

Amplifier simulation results are illustrated in Figure 25. Input return loss is ≤ -18 dB in band, output return loss is ≤ -9.5 dB, and transfer function S21 shows minimum gain 13.7 dB and in band flatness of 0.85 dBpp.

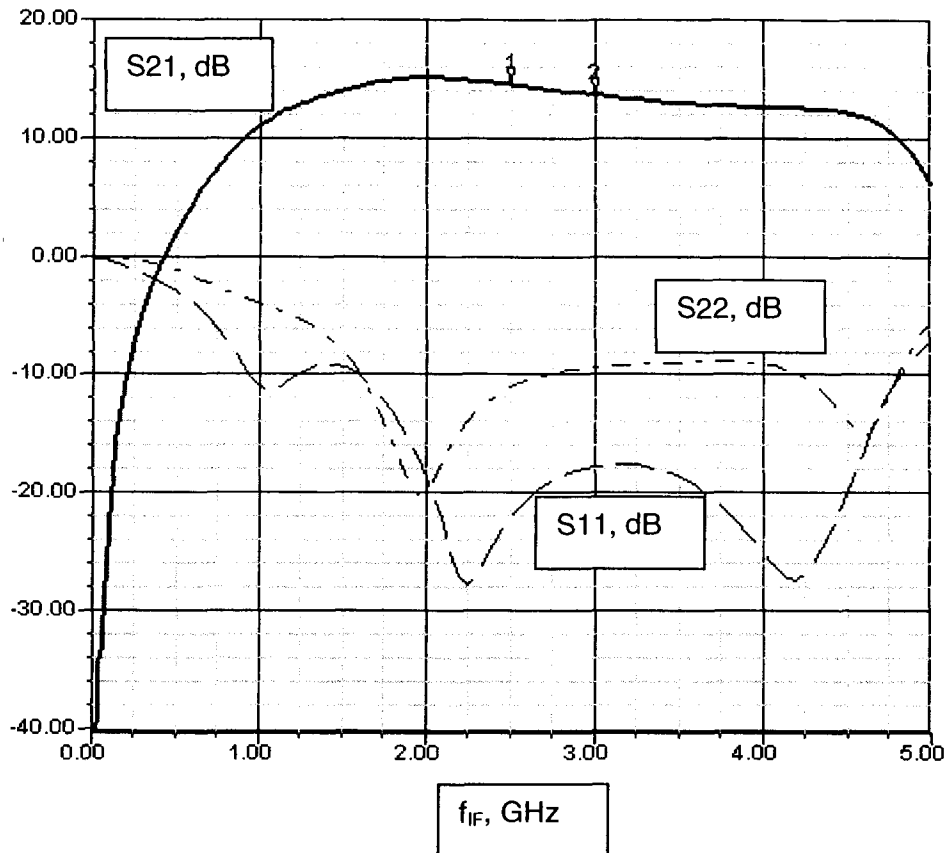


Figure 25: Simulated input/output return loss and S21 transfer characteristics of the amplifier A1.

3.3.2.1.7 Equalizer EQ

Amplifier A1 is followed by amplitude equalizer section. Equalizer function is to optimize overall frequency response and compensate amplitude roll-off caused by amplifiers A1 and A2, and other circuits in the upconverter signal path.

EQ is designed as a band-pass shunt nonconstant-impedance type amplitude equalizer, described by Williams [13], with tunable resonant frequency from 2.35 to 3.25 GHz. Shunt parallel resonant circuit is built using distributed capacitor (low impedance microstrip line) and distributed inductor to ground (high impedance microstrip line shorted at the end using via to ground). The equalizer circuit is illustrated in Figure 26. The amount of correction (0.2 to 2 dB), or maximum insertion loss, is adjusted by selecting resistor R1. This circuit can compensate positive or negative slope, or dip in the middle of the band, by setting resonant frequency of shunt parallel resonant circuit to the lower or higher edge of the band, or in the middle of the band.

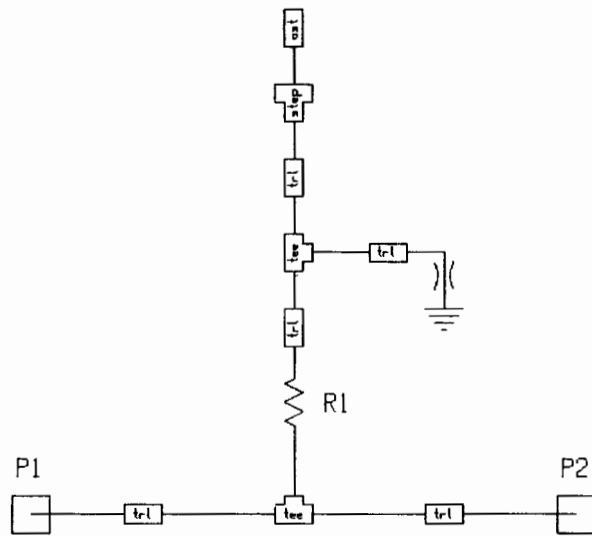


Figure 26: Schematic diagram of the band-pass shunt nonconstant-impedance type amplitude equalizer.

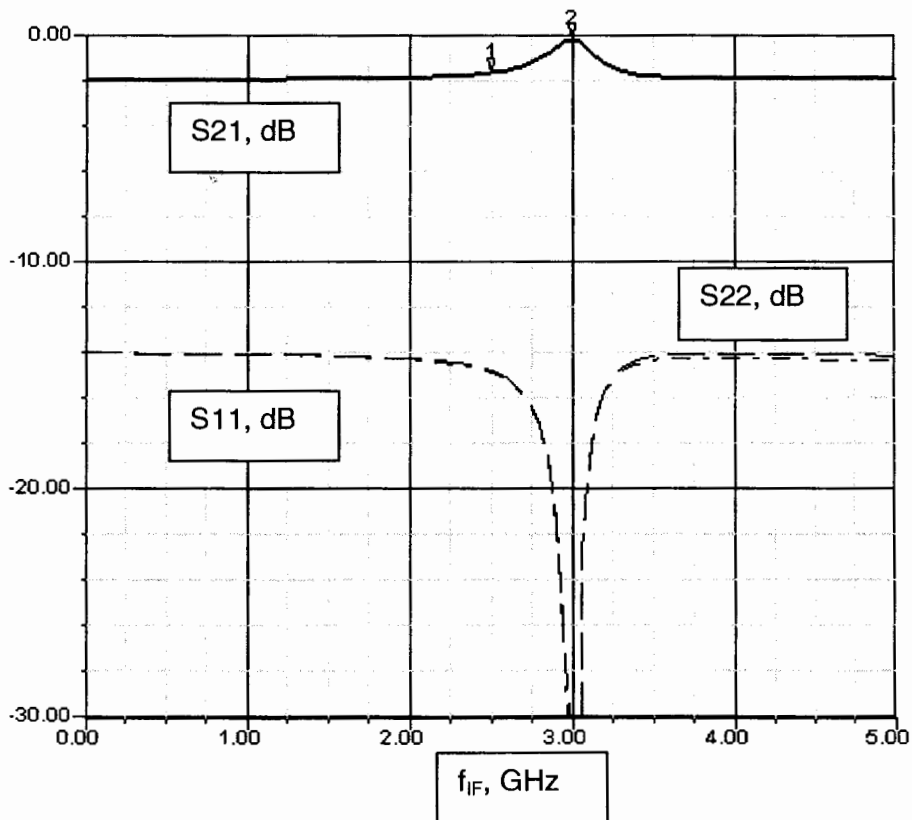


Figure 27: Simulated input/output return loss and S21 transfer characteristics of the equalizer stage with resonant frequency set to 3 GHz.

Figure 27 shows equalizer simulation results with resonance set to 3 GHz. Input/output return loss is ≤ -14 dB in band, and transfer function S21 shows a positive slope of 1.52 dB per 500 MHz.

3.3.2.1.8 Amplifier A2

Sirenza Microdevices [12] SGA series, DC-4.5 GHz, SiGe HBT MMIC amplifier is used as the second gain block. Good return loss, low noise figure ($NF \leq 3.3$ dB) and output IP3 of >31 dBm (with 4 V / 75 mA bias), are the main characteristics of this device. The amplifier schematic with surrounding circuits is identical to amplifier A1 schematic. All design considerations expressed in amplifier A1 description are also valid for amplifier A2. The amplifier simulation results are illustrated in Figure 28. The input return loss is ≤ -16 dB in band, the output return loss is ≤ -11 dB, and transfer function S21 shows minimum gain 11.3 dB and in band flatness of 0.51 dBpp.

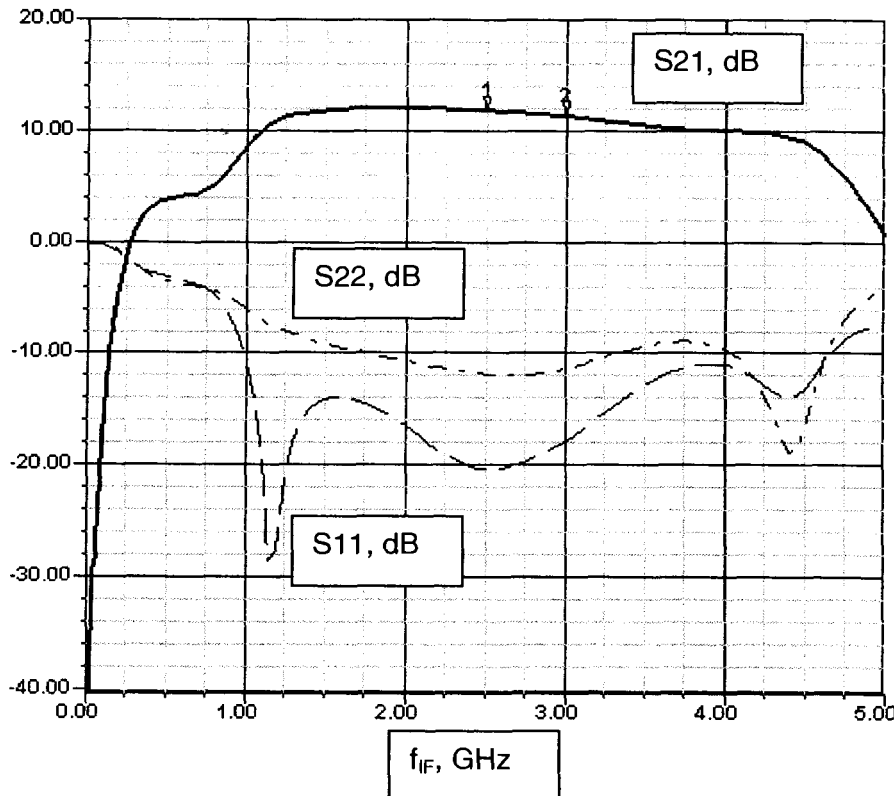


Figure 28: Simulated input/output return loss and S21 transfer characteristics of the amplifier A2.

3.3.2.1.9 Attenuator ATT3

5 dB, 50 Ω , T attenuator is placed at the end of the IF chain, to improve matching between amplifier A2 and mixer section and to bring IF section gain to desired level.

Schematic diagram is similar to schematic diagram of the attenuator ATT1.

This concludes the description of the intermediate frequency stage.

Figure 29 shows IF section simulation results. Input return loss is ≤ -19.5 dB, output return loss is ≤ -22 dB, and transfer function S21 shows minimum gain of 14.48 dB and in band flatness of 0.56 dBpp.

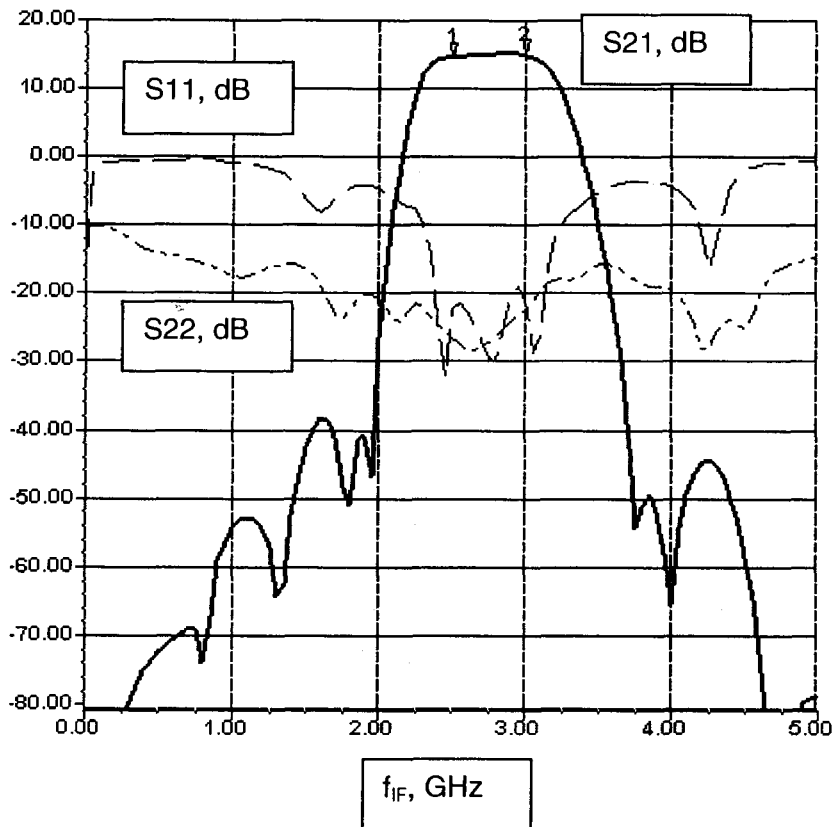


Figure 29: Simulated input/output return loss and S21 transfer characteristics of the intermediate frequency stage.

3.3.2.2 Mixer Stage

The mixer stage takes the intermediate frequency signal and converts it to output RF signal (29.5 to 30 GHz), using the local oscillator signal from LO circuitry. The main goal is to design a mixer with high output power capabilities (1dB compression point or IP3), as that decreases the required gain at Ka frequencies, which is equivalent to number of required Ka amplifier stages.

Two mixer versions are considered below, FET resistive mixer and chip sub-harmonic MMIC mixer.

3.3.2.2.1 GaAs FET Resistive Mixer

This resistive mixer, which uses the channel resistance of an unbiased GaAs FET to perform frequency mixing (down-conversion) at X band (10 GHz), is described by Mass [14]. The principles depicted in his paper are used to design a 30 GHz mixer for upconversion.

The unbiased channel operates as a resistor controlled by the gate voltage in the FET's I/V curve region commonly called *linear*. Since this resistance is weakly nonlinear, the mixer generates low intermodulation, hence it is capable of delivering high output power with moderate LO levels.

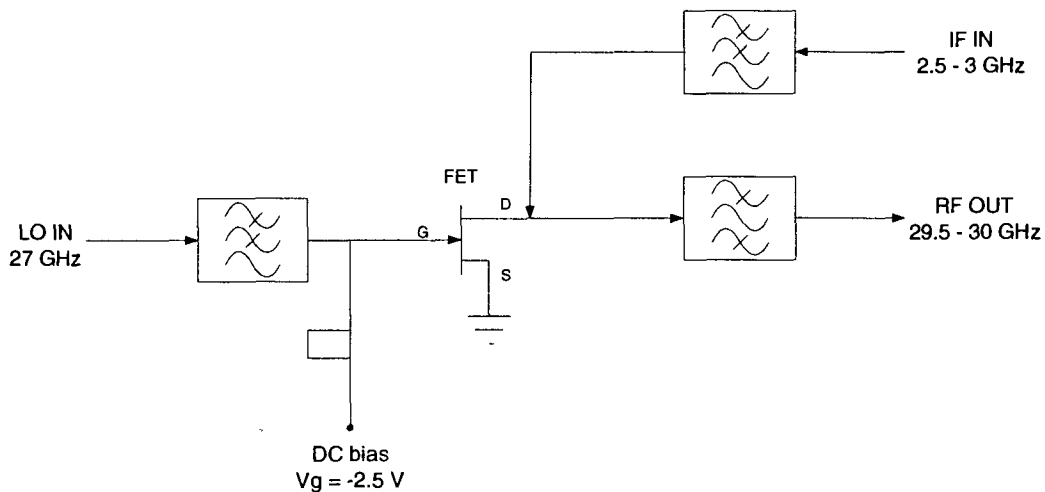


Figure 30: Block diagram of the resistive FET mixer.

The mixer realization is presented in Figure 30. The FET operates in a common-source configuration; the LO and negative bias are applied to the gate, and IF is applied to the drain. The RF signal is then filtered from the drain. The RF/IF filters are designed to short-circuit the drain at LO frequency, to prevent LO voltage coupling to the drain, which will cause operating point translation in more nonlinear region. LO filter (matching circuit) is designed to short-circuit the RF signal at the gate, and prevent intermodulation.

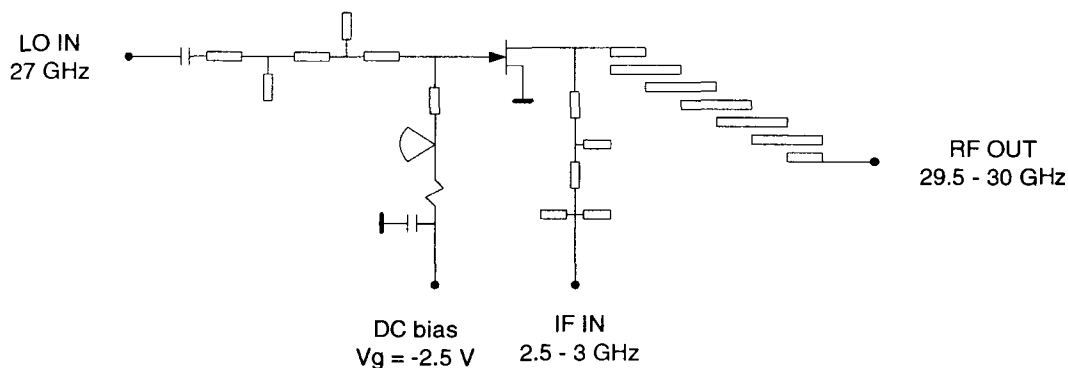


Figure 31: Schematic diagram of the resistive FET mixer.

The mixer consists of NEC [15] NE32400 die FET and three filters; see Figure 31 for details. Required filters are first designed, and then put together with FET nonlinear model.

The NE32400 is a Hetero-Junction FET with pinch-off voltage between -2V and -0.2V , when biased ($V_{ds}=2\text{V}$). The packaged FET cannot be used since package parasitics at 30 GHz are destroying response characteristics. The RF filter is a 5th order, Edge Coupled Half Wave microstrip band-pass filter, with $BW_{1\text{dB}}=1.2\text{GHz}$ and 2.5 to 2.75 dB insertion loss in a pass band (29.5 to 30 GHz), in 50 Ω system. The IF filter is a 4th order Elliptical microstrip filter, with cut-off frequency of 5 GHz, insertion loss of 0.35 dB in band (2.5 to 3 GHz), and poles positioned at 27 GHz and 29.75 GHz. The LO filter is a simple two stub design, tuned to match the LO source to gate input impedance.

With the LO drive of +10 dBm, gate bias is adjusted for minimum conversion loss and best IF port match ($V_g = -2.5\text{V}$). The Ansoft Serenade simulation tool is used to perform nonlinear simulation and tuning.

Figure 32 demonstrates the simulated output spectrum. Mixing product analysis and nonlinear simulation shows that the components closest to the band of interest are 2LO (27 GHz) and 2LO+2IF (32 – 33 GHz). Undesired in-band mixing products, with

order <10, are not found. The achieved conversion loss of 10.6 dB maximum, and flatness of 0.46 dB, is shown in Figure 33.

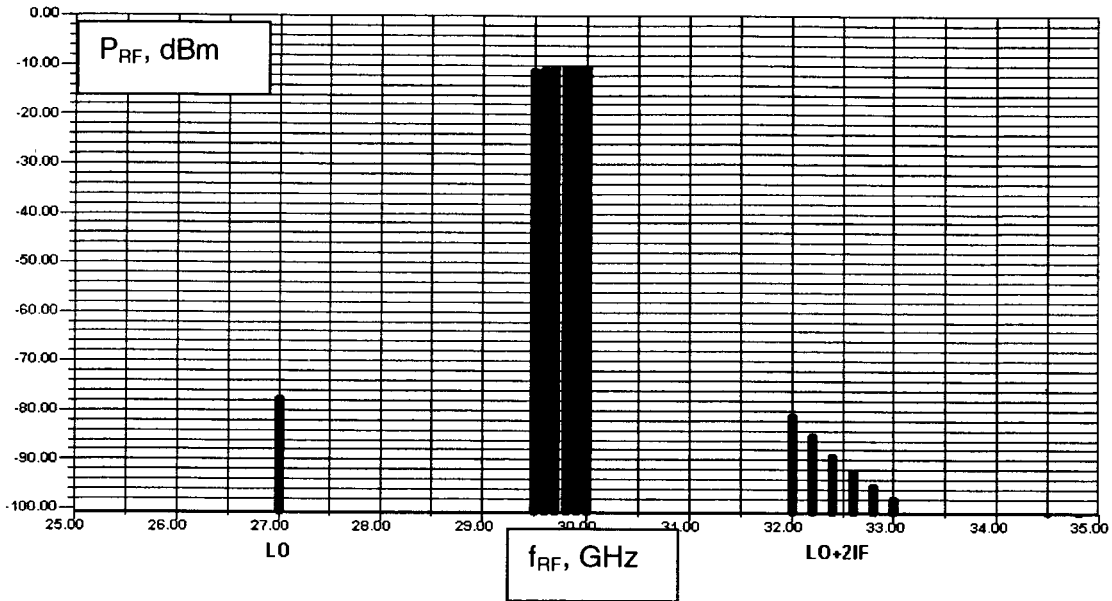


Figure 32: Simulated mixer RF output power as a function of RF frequency.

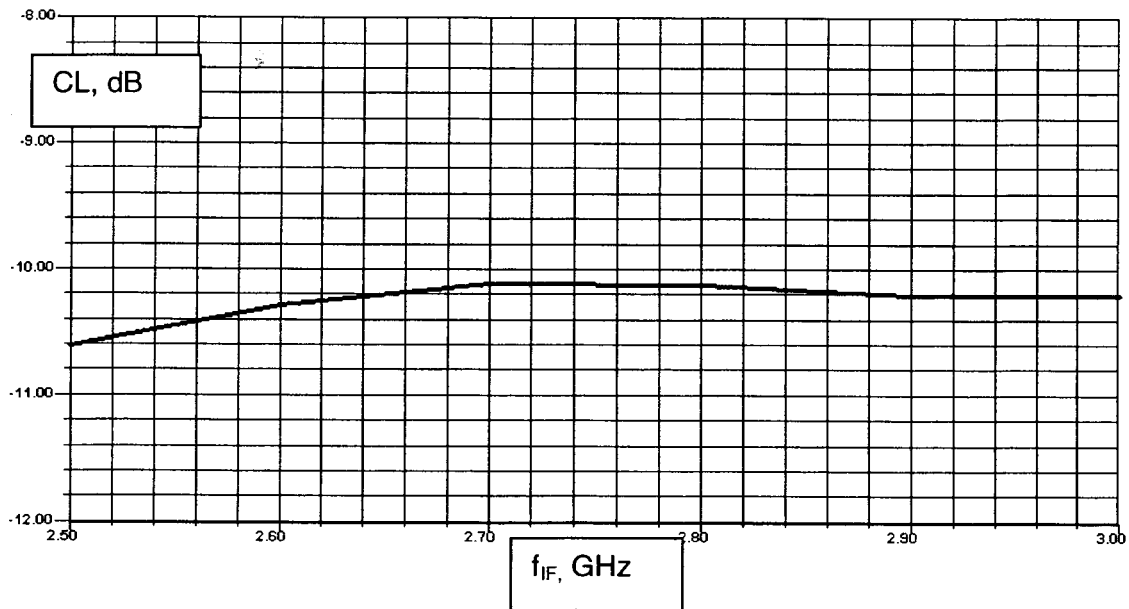


Figure 33: Simulated mixer conversion loss as a function of IF frequency.

Figure 34 shows the compression characteristic of the mixer as sinusoidal IF power is swept (from -20 to +20 dBm). P1dB input compression point is +6 dBm and P1dB output compression point is -4.15 dBm. Figure 35 shows input impedances on all three ports.

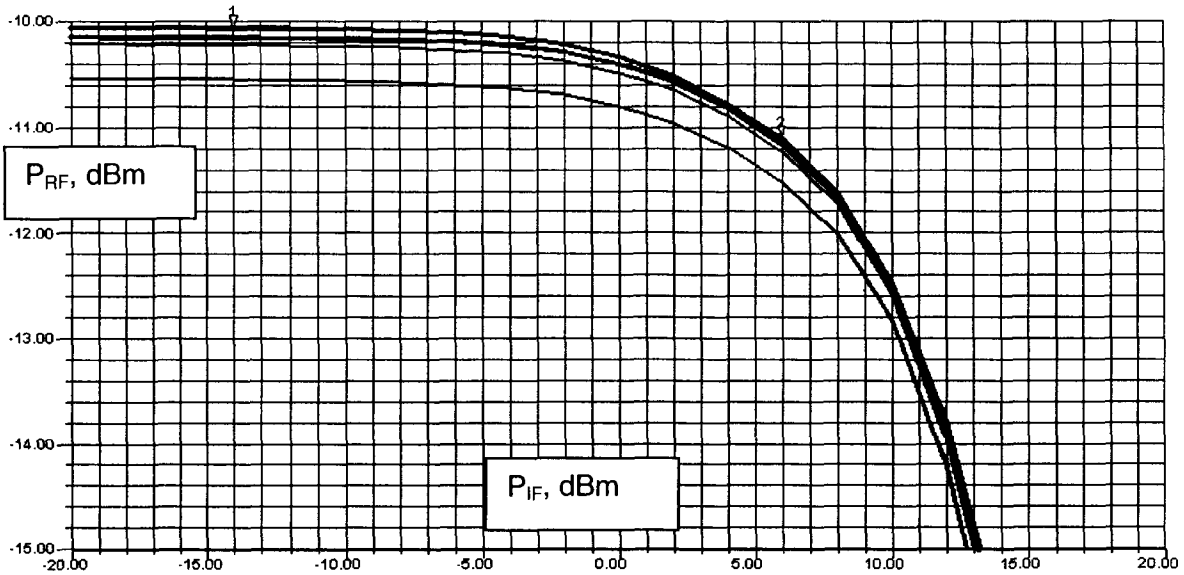


Figure 34: Simulated mixer compression characteristic – output RF power as a function of input IF power.

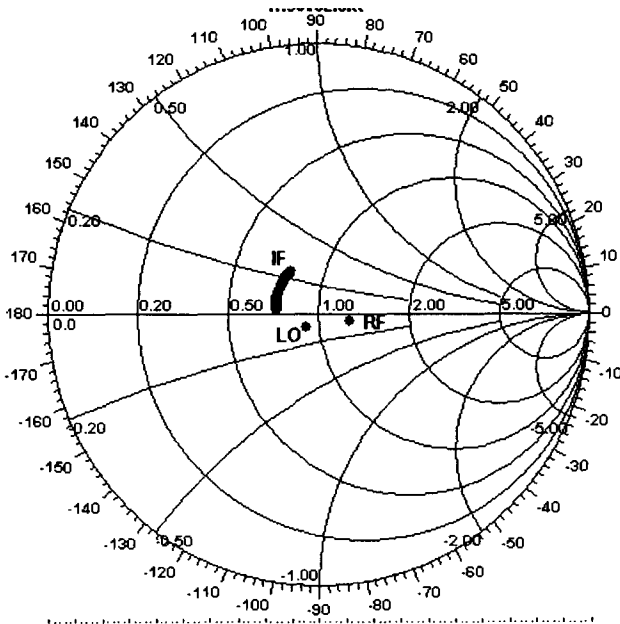


Figure 35: Simulated input impedances of the IF, LO and RF port.

3.3.2.2.2 Sub-harmonic MMIC mixer

A Hittite [16] chip sub-harmonically pumped mixer with an integrated LO amplifier is used to upconvert IF signal to Ka band ($RF = 2LO + IF$). Since this is a sub-harmonic mixer, a 13.5 GHz LO signal is required for conversion. The integrated LO amplifier is single biased (+4V), dual stage design, so only -4 dBm LO drive is necessary. A GaAs PHEMT technology is utilized in the MMIC design, resulting in a small chip size (0.97 x 1.32 mm).

Other mixer parameters are:

- RF Frequency Range: 24 – 32 GHz
- LO Frequency Range: 12 – 16 GHz
- IF Frequency Range: DC – 6 GHz
- Conversion Loss: 10 dB typ.
- 1 dB compression out: -4 dBm typ.
- 2LO to RF Isolation: 35 dB typ.
- LO power: 0 dBm

Mixing product analysis shows that components closest to the required band are $2LO$ (27 GHz) and $2LO + 2IF$ (32 – 33 GHz). In addition, 7th order in band mixing spurious, $3LO - 4IF$ (30.5 – 28.5 GHz) and $LO + 6IF$ (28.5 – 31.5 GHz), are discovered.

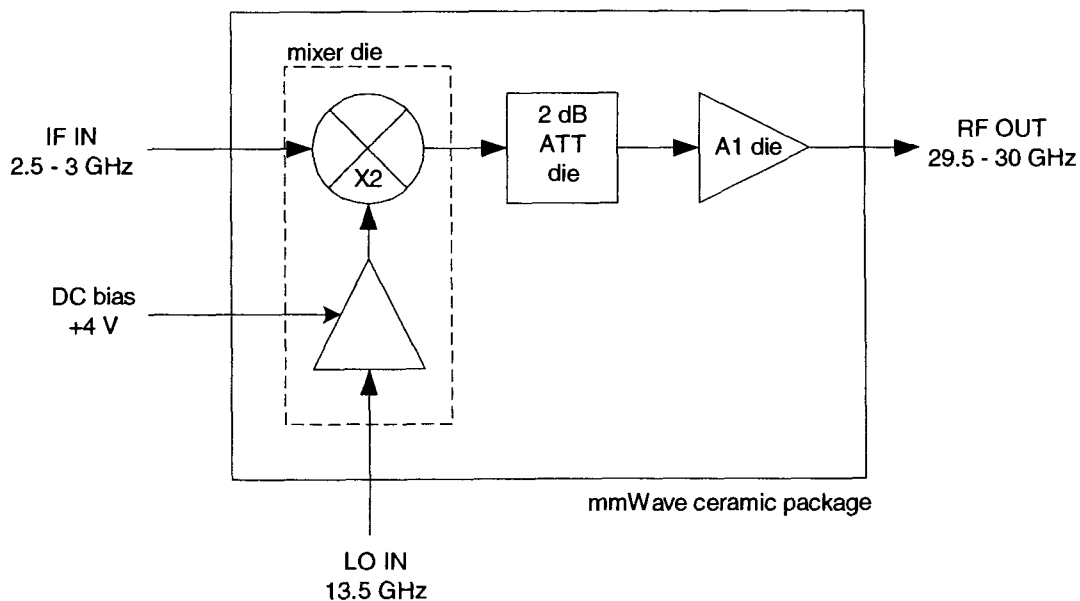


Figure 36: Block Diagram of the MMIC Mixer section.

Mixer die, combined with 2dB attenuator die and amplifier die, is packaged in the ceramic mmwave package. This package is then attached to printed circuit board where it is interfaced with the IF board, LO board and output band-pass filter, using 50 W microstrip transmission lines.

A1 is a two-stage wide band (20 to 30 GHz), monolithic low noise (3 dB maximum) amplifier with 13 dB gain and flatness of 2 dBpp. The amplifier is placed between the mixer output and the band-pass filter input, to improve isolation and offer broader matching to mixer RF port.

To conclude, the two mixers under consideration have similar conversion loss and power handling capabilities (P1dBcp), and require a clean room environment for assembly. The MMIC mixer is implemented since it has smaller size, lower LO frequency (13.5 compared to 27 GHz) and LO power requirement (0 dBm compared to +10 dBm).

3.3.2.3 Output Band-pass Filter

The 5th order Finline band-pass filter (BPF) is the next stage in the upconverter chain. The main BPF task is to filter upper side mixing band (2LO+IF) and to reject 2LO (27 GHz) and 2LO+2IF (32 to 33 GHz) signals and other undesired mixing products.

The main filter requirements are:

- 1dB Pass band: 29.3 – 30.2
- Insertion Loss: ≤ 3 dB
- Input/Output Return Loss: > 15 dB
- Rejection @ 27 GHz > 60 dB
- @ 32 GHz > 40 dB

3.3.2.4 Solid State Power Amplifier Module

The solid-state power amplifier (SSPA) module is a multi-stage unit whose main function is to amplify microwave signals to the desired +32 dBm (1dBcp) output power.

GaAs MMIC amplifiers, designed for 50 Ω system, are used as building blocks. MMIC chips are first die-attached and wire-bonded into ceramic mm-wave packages, in a clean room environment, and then assembled with printed circuit board to the

aluminum sub-base plate. Altogether there are four packages inside the SSPA module. Package 1 contains the low noise MMIC amplifier die (LNA). Package 2 holds the LNA with integrated variable attenuator used for module temperature compensation. Package 3 contains the driver MMIC amplifier with P1dB around +23 dBm. Package 4 carries the power amplifier pair in a balanced configuration. Each of the power amplifier MMICs has P1dB of +30 dBm. At the end of the amplifier chain, the microwave signal is launched into WR28 wave-guide. Figure 37 presents SSPA block diagram.

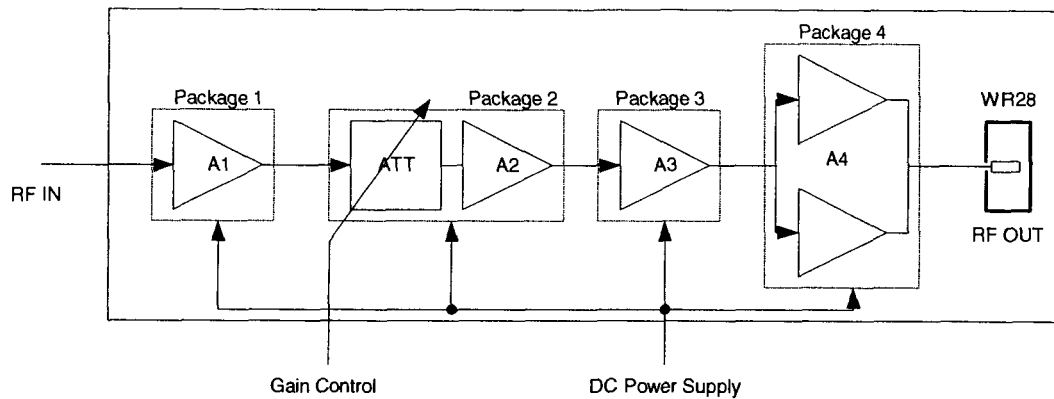


Figure 37: Block diagram of the solid-state power amplifier section.

Other module parameters are:

- Frequency range: 25 – 30 GHz
- Gain at 25 deg. C (att=0dB): 60 ± 1 dB
- Gain Variation Over Temperature: 14 dB
- Output P1dBcp: ≥ 32 dBm
- Gain Tuning Range: > 15 dB
- Input Return Loss: > 12 dB
- Output Return Loss: > 8 dB

3.4 Measurement Results

The measurement results of the upconverter sub-circuits, as well as the unit level results are presented in this section.

3.4.1 Sub-circuit Level Measurement Results

3.4.1.1 *intermediate Frequency Section*

Figure 38 presents the measurement setup used during the IF section evaluation measurement. Since the IF input impedance is $75\ \Omega$, a $50\text{-}75\ \Omega$ minimum loss pad is used to transform Network Analyzer $50\ \Omega$ impedance (port P1) into $75\ \Omega$. The pad output is then calibrated using a $75\ \Omega$ calibration kit. Calibration is also performed at the end of cable from port P2, using a $50\ \Omega$ coaxial calibration kit.

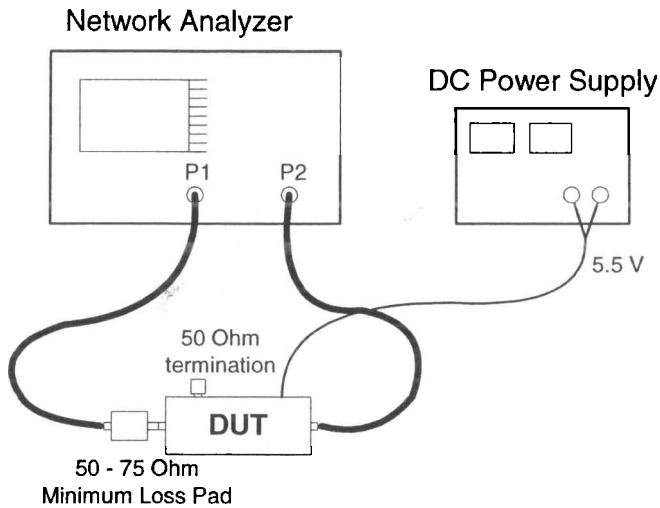


Figure 38: Measurement setup diagram of the intermediate frequency section.

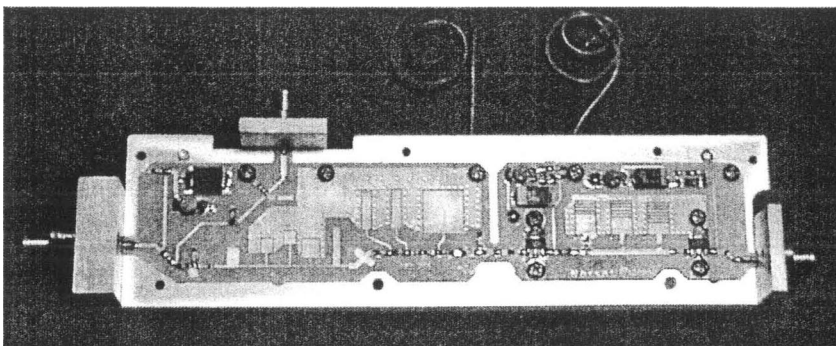


Figure 39: Test Jig used for measurement of the intermediate frequency section.

Figure 39 shows the Test Jig used to secure the IF PCB, and to provide an interface to measurement equipment. Figures 40 shows IF section measured input return loss (S11) as a function of frequency. Desired frequency range is between marker 1 (2.5 GHz) and marker 2 (3GHz). Result is consistent with the simulation. Worst-case return loss result of -17.1 dB is recorded at 3 GHz frequency.

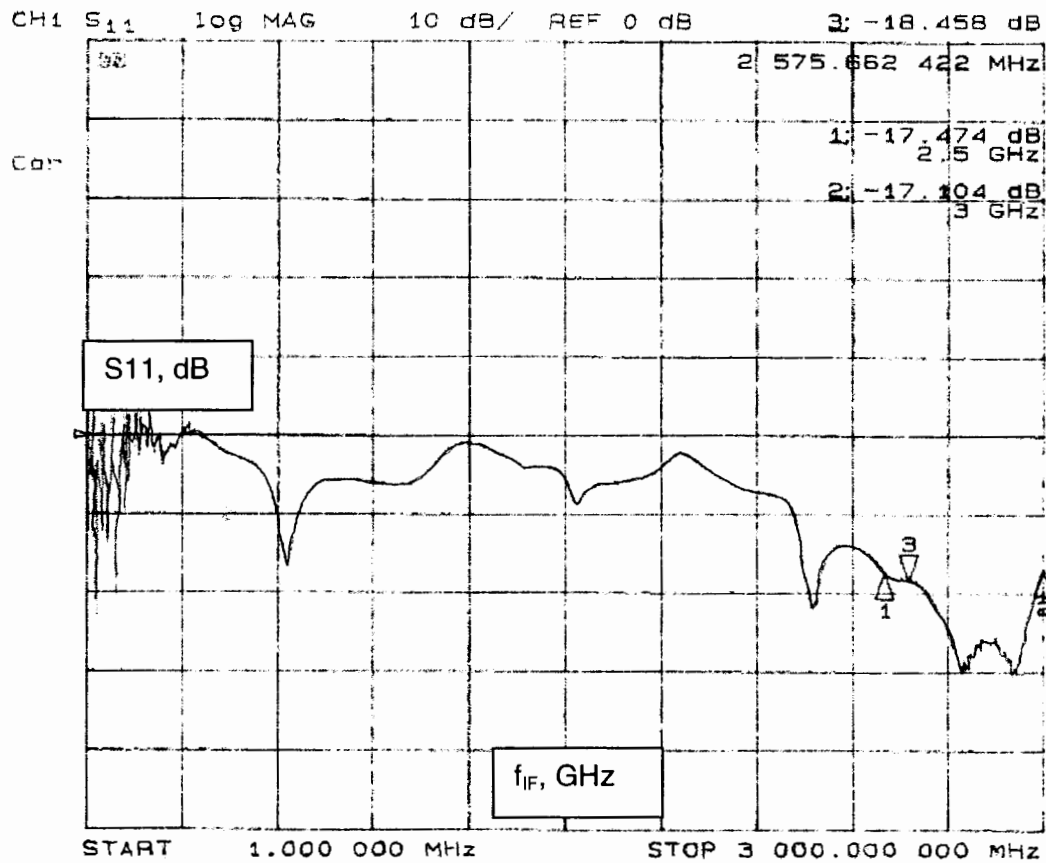


Figure 40: Measured input return loss of the intermediate frequency section (10 dB per division scale).

Figure 41 shows IF section measured output return loss (S22) as a function of frequency. Desired frequency range is between marker 1 (2.5 GHz) and marker 2 (3GHz). Worst-case return loss result of -19.565 dB is recorded at 2.728 GHz frequency (marker 3).

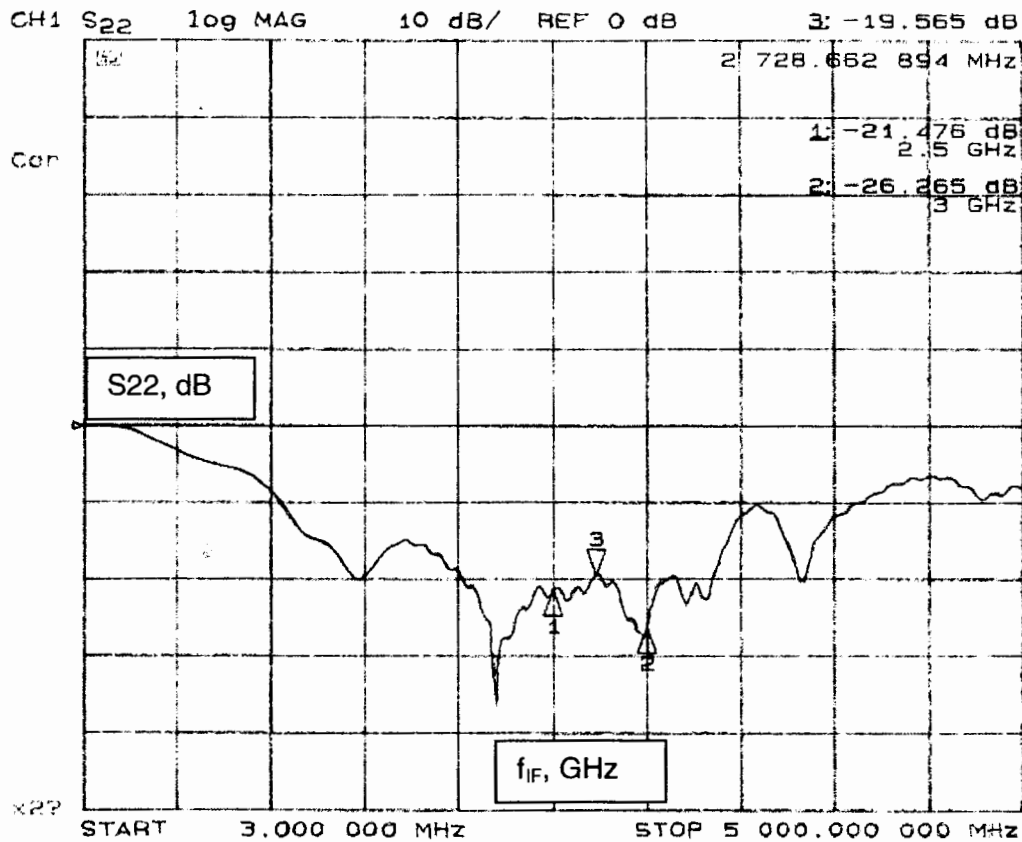


Figure 41: Measured output return loss of the intermediate frequency section (10 dB per division scale).

Figures 42 and 43 demonstrate the IF section transfer characteristics as a function of frequency. General shape and pole positions are very close to simulation (see Figure 29). A minimum gain of 13.57 dB and flatness of 0.34 dBpp, are recorded.

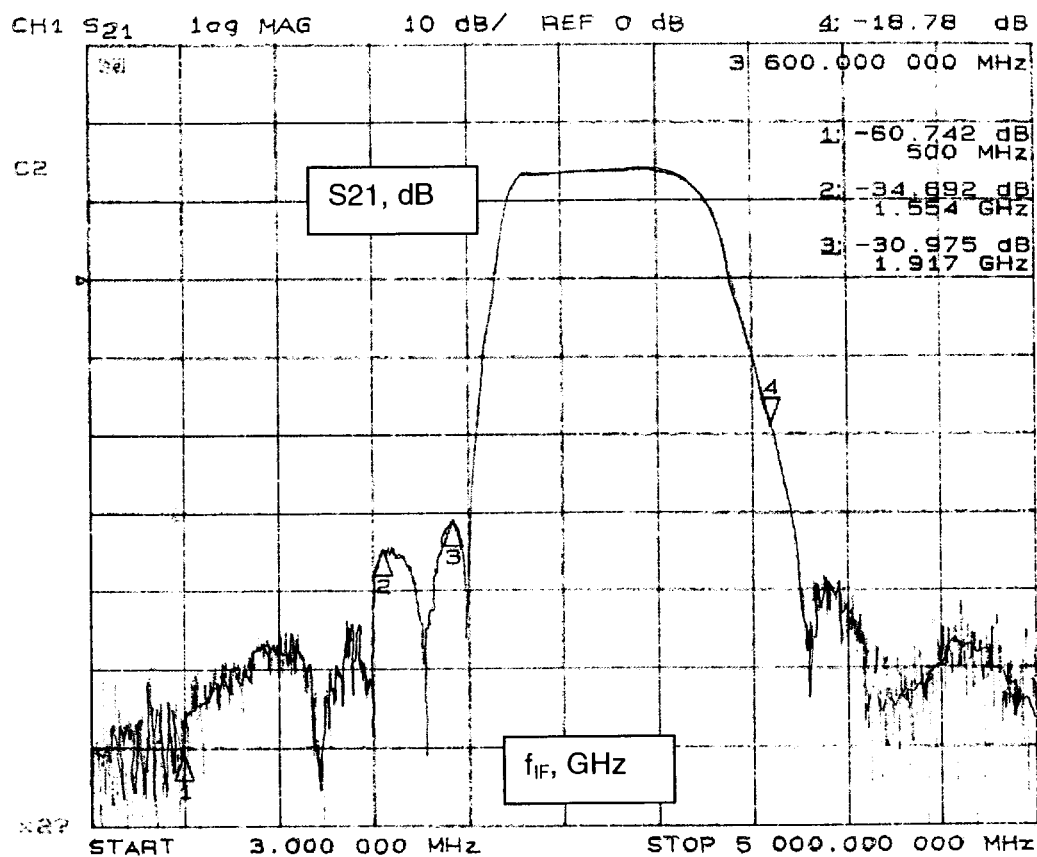


Figure 42: Measured intermediate frequency section transfer function S21 as a function of frequency (10 dB per division scale).

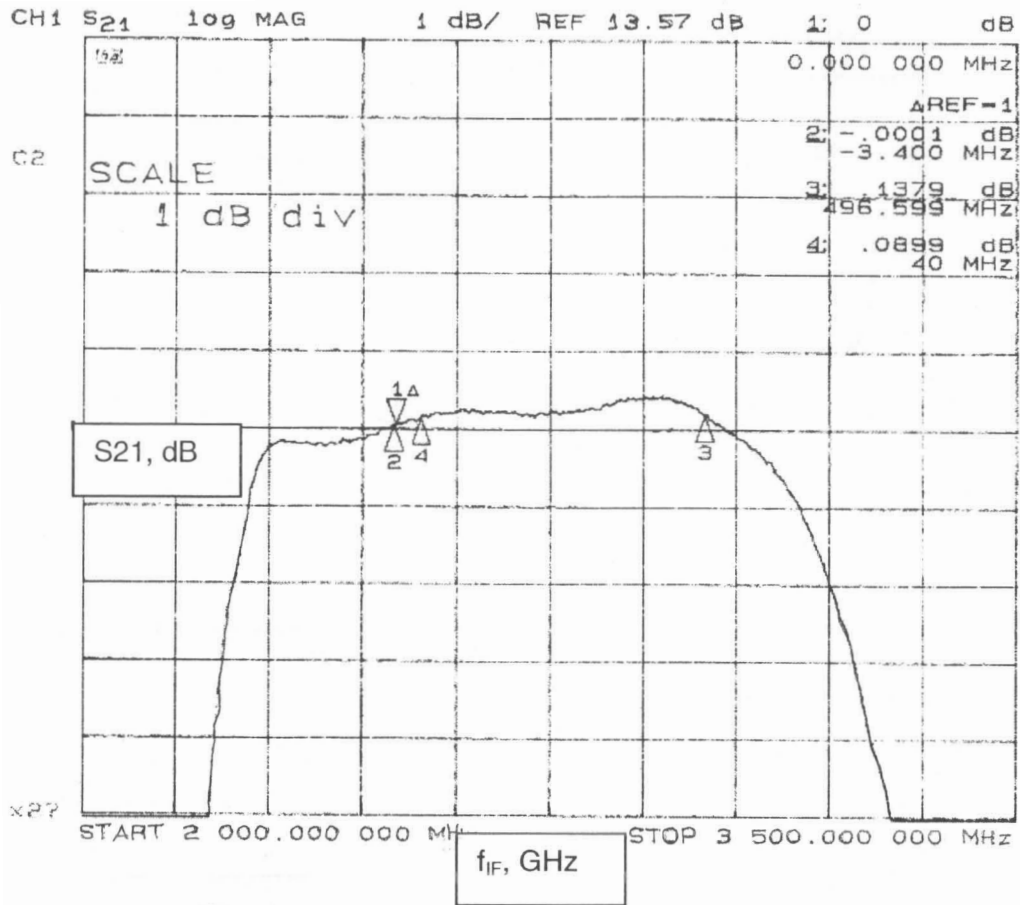


Figure 43: Measured intermediate frequency section transfer function S_{21} as a function of frequency, with 1 dB per division scale.

3.4.1.2 Mixer

Figures 44 and 45 show the mixer test jig and equipment setup diagram used for circuit evaluation.

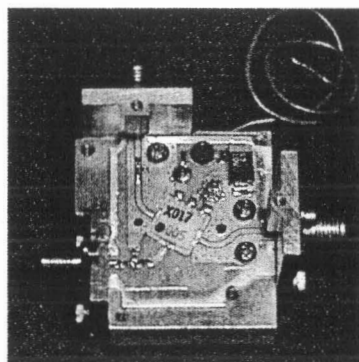


Figure 44: Test jig used for measurement of the mixer section.

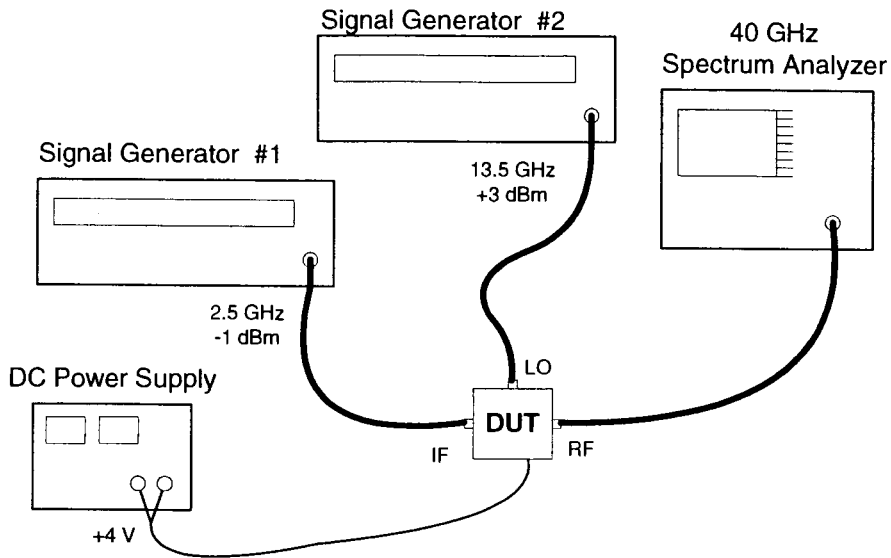


Figure 45: Measurement setup diagram of the mixer section

The spectral content at the mixer RF port, with injected IF frequency of 2.5 GHz, is presented in Figure 46. The closest spurious signals, $2LO$ and $2LO+2IF$ are -2 dBc and -35 dBc, respectively, below the desired 29.5 GHz signal.

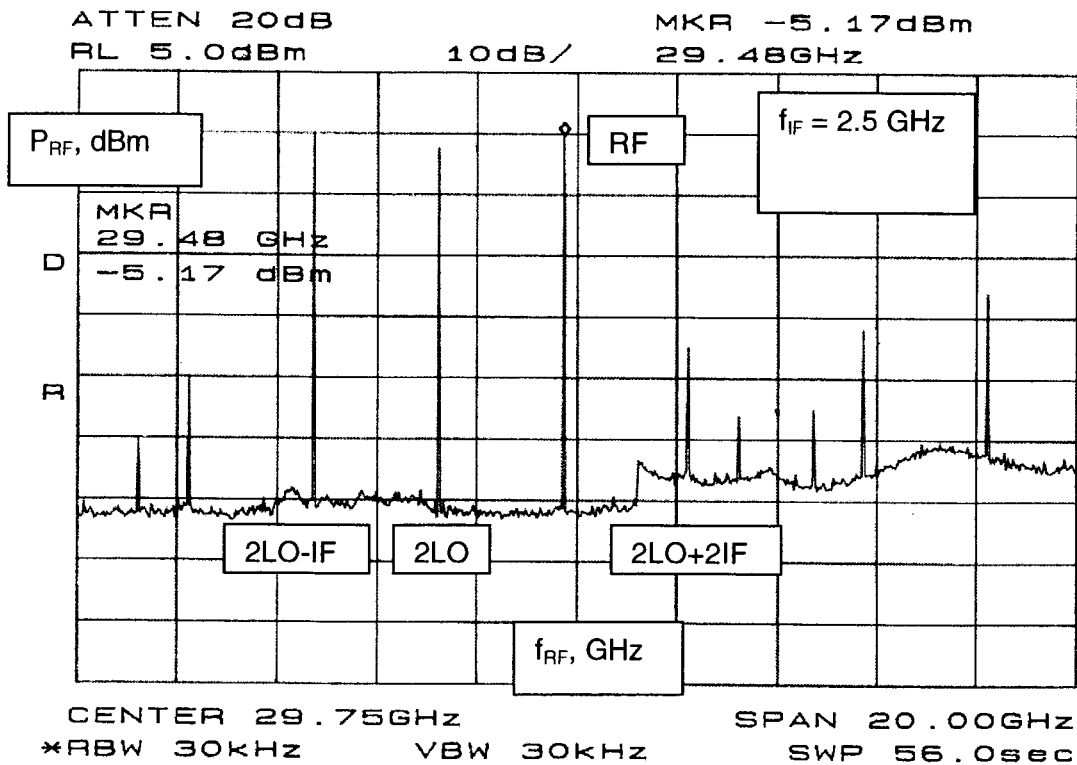


Figure 46: Measured mixer RF port power spectrum as a function of frequency.

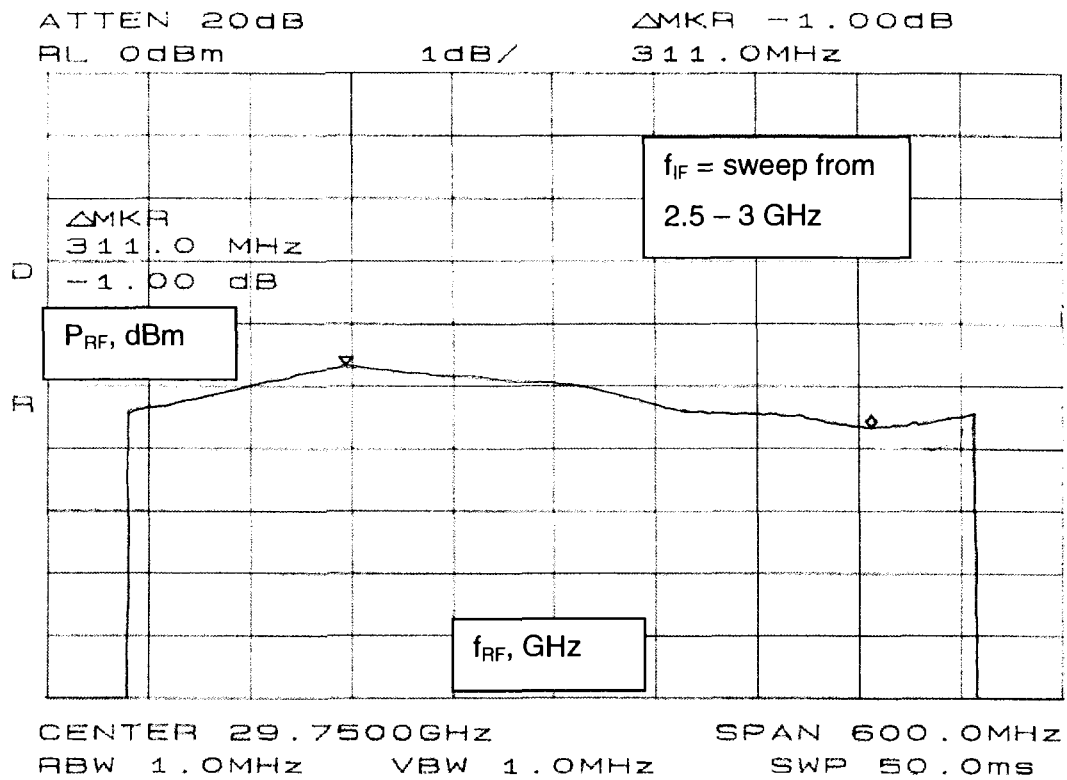


Figure 47: Measured mixer RF output power variation as a function of frequency (1 dB per division scale).

To produce the conversion loss response illustrated in Figure 47, the IF signal generator is swept from 2.5 to 3 GHz. A flatness of only 1 dB, in full 500 MHz band, is recorded. Delta marker spectrum analyzer function is used to measure difference between maximum and minimum power level.

3.4.1.3 Band-Pass Filter

A 40 GHz Network Analyzer is used to evaluate Finline filter performance. Measurement cables are calibrated prior to measurement. Figure 48 shows the equipment setup.

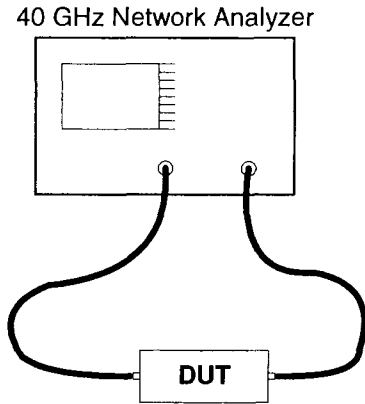


Figure 48: Measurement setup diagram of the band-pass filter section.

Input return loss graph, as a function of frequency, is presented in Figure 49. Worst case result of -12.4 dB at 30 GHz is recorded.

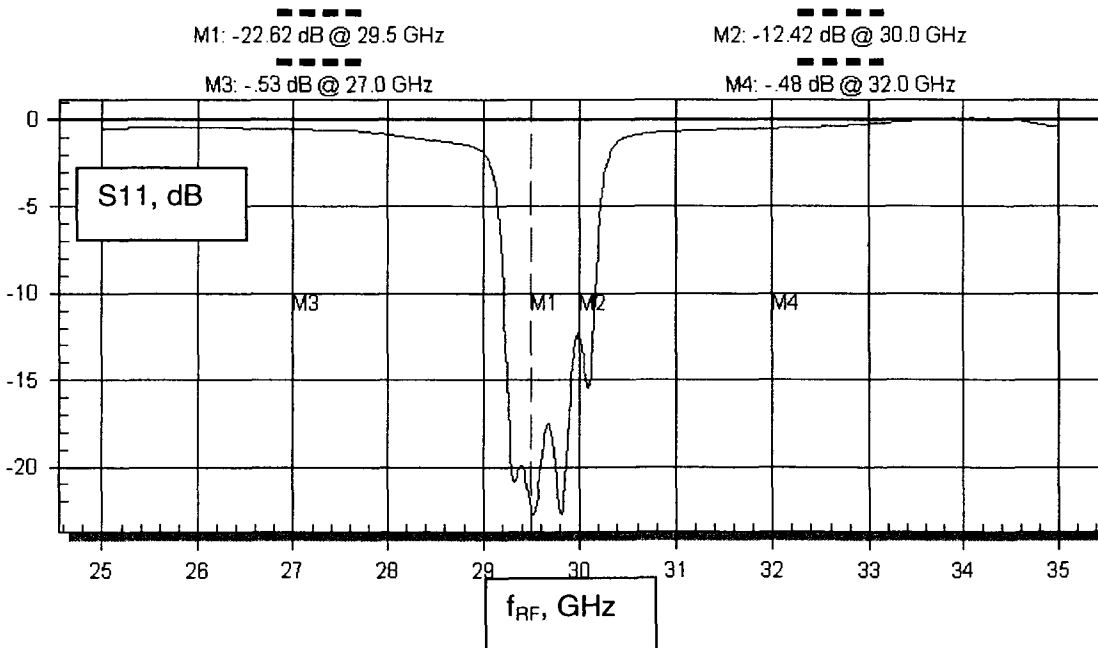


Figure 49: Measured filter input return loss as a function of frequency.

The filter frequency response is shown in Figure 50. Insertion loss of only 2.3 dB is recorded (between markers M1 and M2). Rejections of more than 70 dB at 27 GHz (marker M3), and more than 50 dB at 32 GHz (marker M4), are more than adequate for the complete elimination of unwanted spurious signals (2LO and 2LO+2IF).

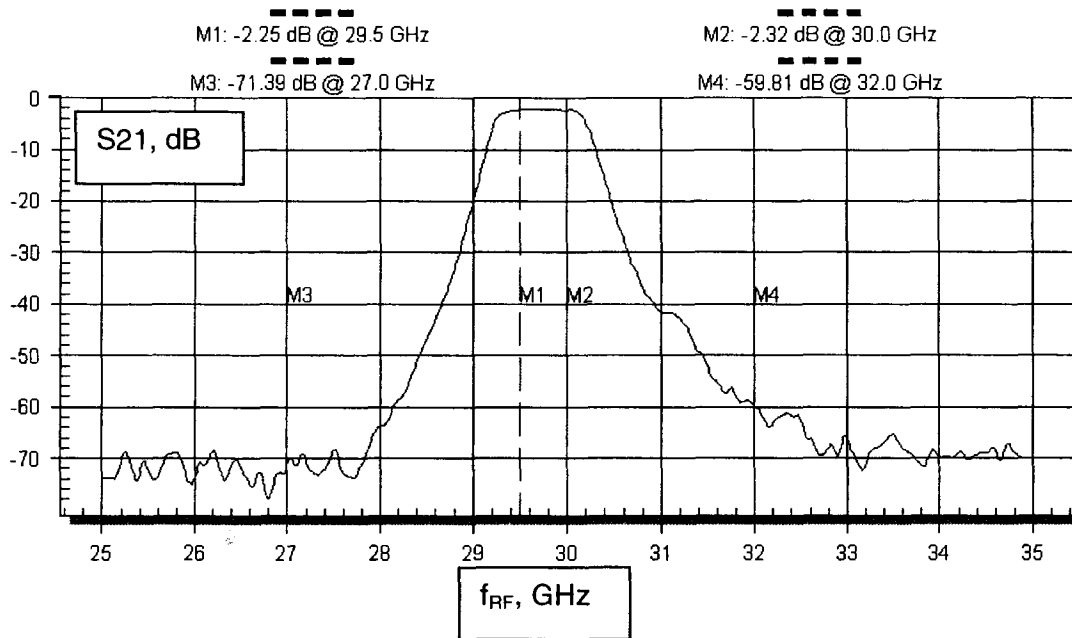


Figure 50: Measured filter transfer function S_{21} as a function of frequency.

3.4.1.4 Solid State Power Amplifier

The solid state power amplifier (SSPA) module was evaluated using the same setup as in Figure 48, with addition of a DC Power Supply.

Figure 51 shows the input and output return loss, forward transfer function and isolation. An input return loss of -13 dB and an output return loss of -8 dB (worst case) are recorded. A maximum gain of 61.5 dB (control voltage set to minimum attenuation) and isolation of more than 80 dB are also measured.

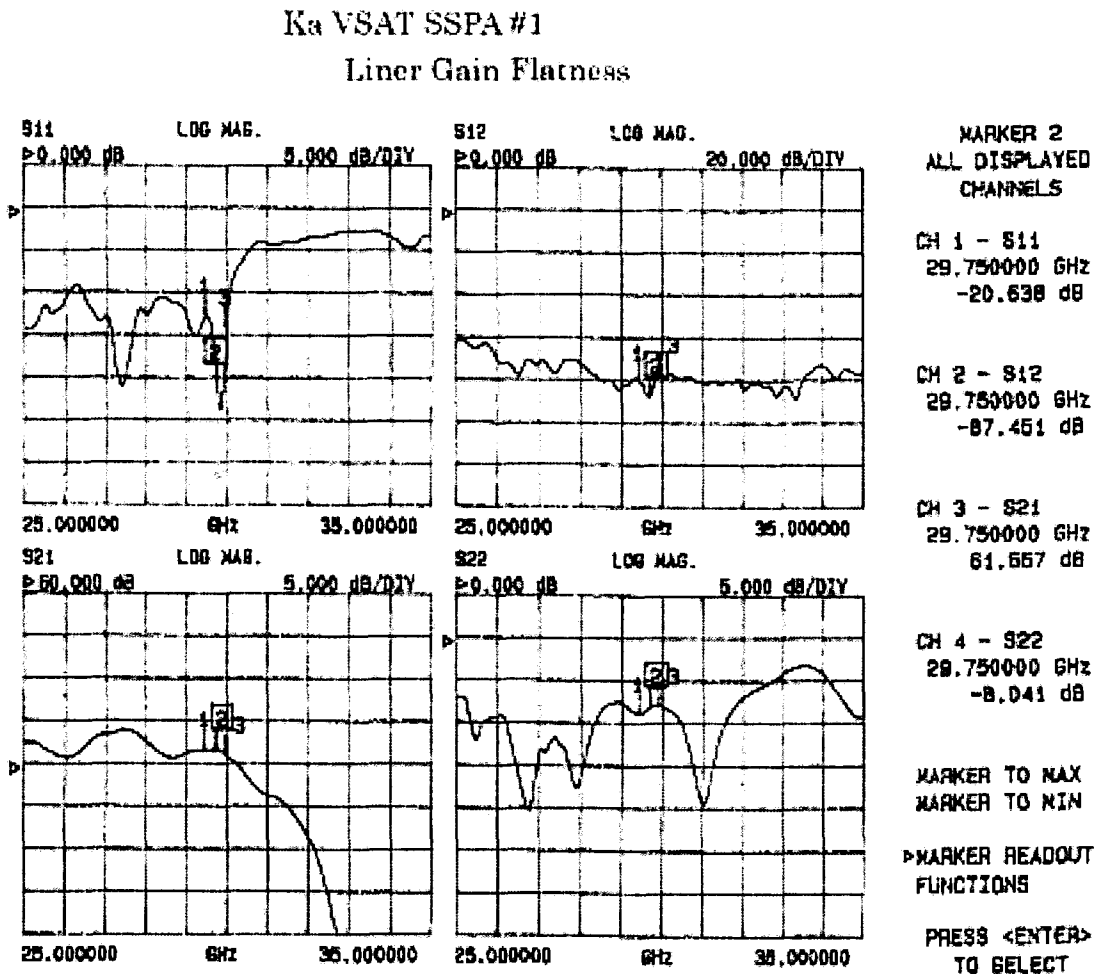


Figure 51: Measured power amplifier input and output return loss (S11 and S22), and forward (S21) and reverse (S12) transfer characteristics, as a function of frequency.

Figure 52 illustrates the input-versus-output power response. The measurement was performed for 29.75 GHz output frequency, with temperatures of -15 to $+65$ deg.C. P1dB measures $+32.8$ dBm at -15 deg. C, and then drops with a temperature increase to $+31$ dBm at $+65$ deg. C.

Gain variation over temperature information can be also extracted from this graph. Gains of 54.8 dB and 65.6 dB are measured at $+65$ and -15 deg. C. Assuming that gain will rise an additional 2.1 dB, from -15 to -30 deg. C, the total gain variation is 13 dB. This variation is inside the range of the variable attenuator integrated with the second amplifier section.

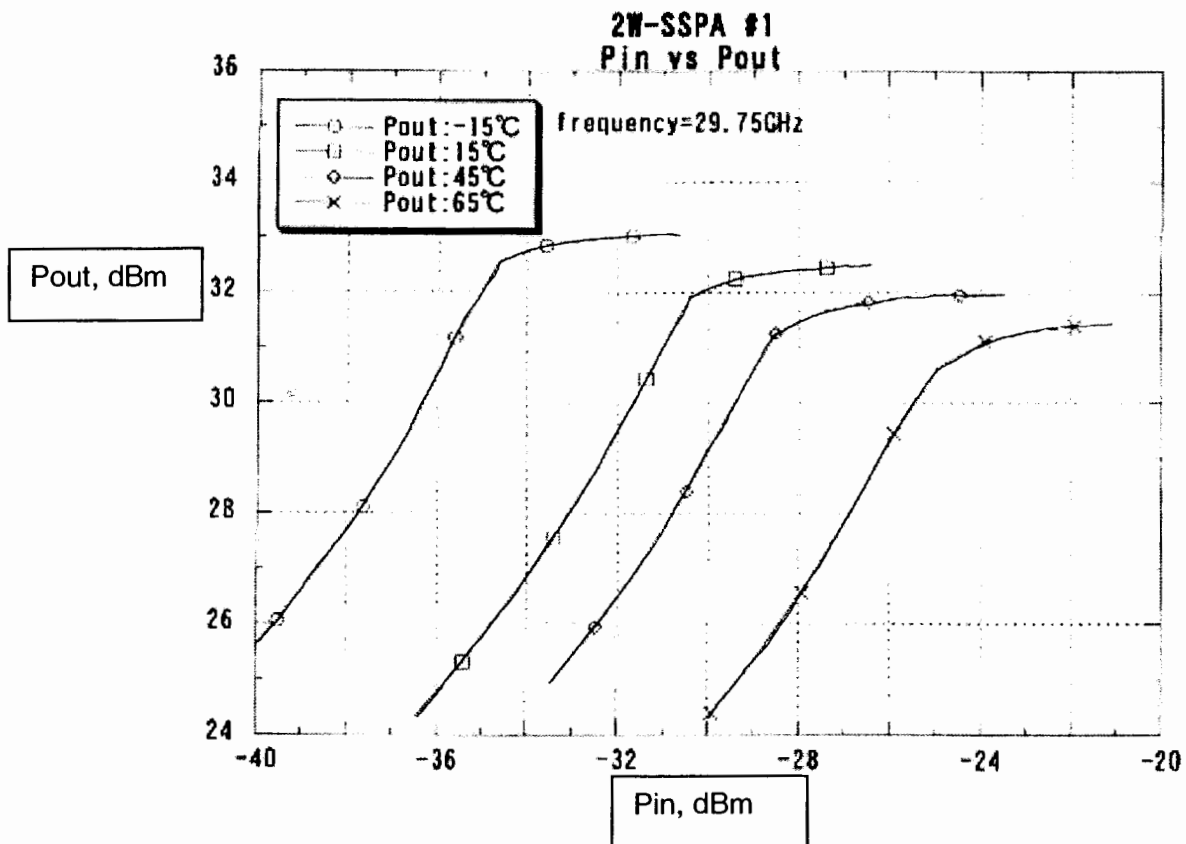


Figure 52: Measured input-versus-output power response, over temperature, for 29.75 GHz signal frequency.

Measurement results of a prototype SSPA module are presented above. Current production modules achieve higher P1dB compression points, due to improvement in matching between the output power amplifier stage and the microstrip to waveguide launch.

3.4.2 Unit Level Measurement Results

Unit level measurement results are collected using Automated Test Equipment (ATE) setup and they are presented in this sub-section.

Figure 53 shows a picture of the transmitter RF section. Beside the upconverter chain, Reference, LO and SSPA Power Supply PCBs are illustrated.

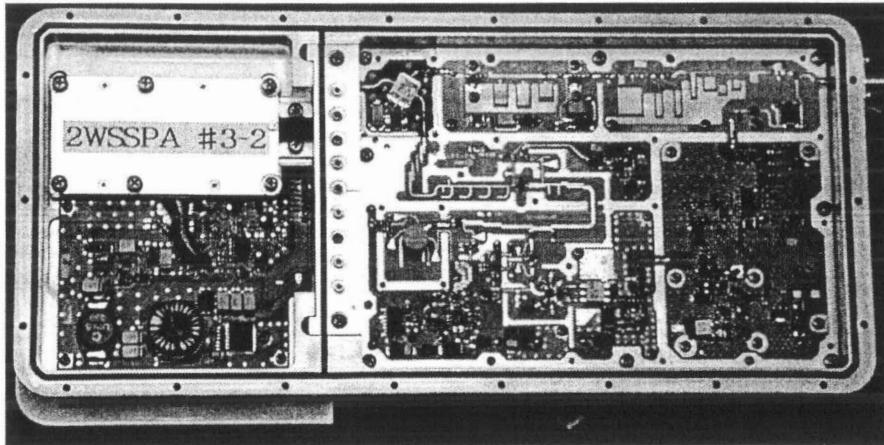


Figure 53: Picture of the Ka-band transmitter RF circuitry.

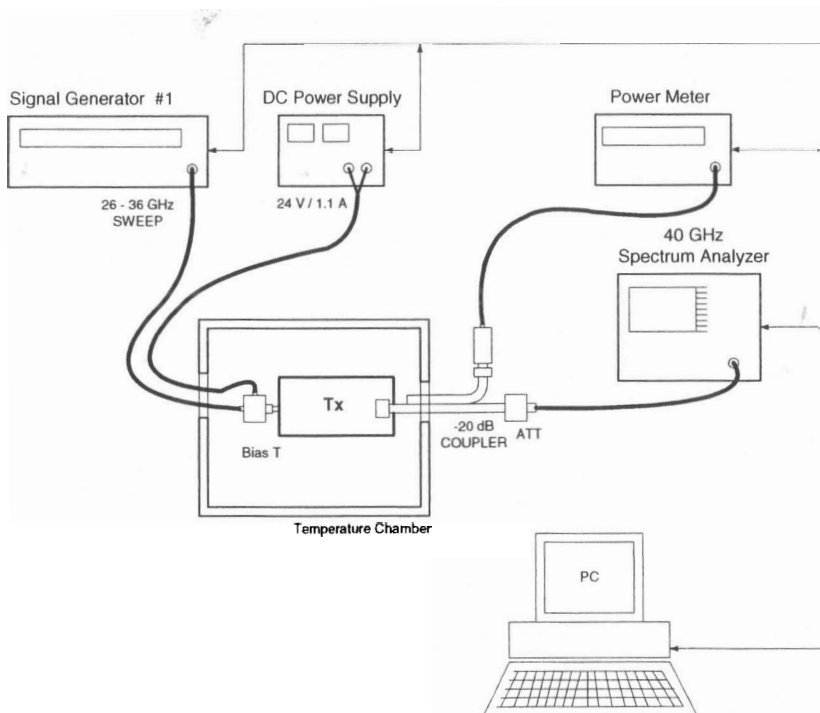


Figure 54: Automated measurement setup diagram of the transmitter unit.

Figure 54 illustrates the ATE measurement setup, which enables completely automated unit evaluation over temperature (-30 to +50 °C). A software application controls all instruments and temperatures via a GPIB interface. The duration of the entire test is approximately 4 hours.

Measured transmitter unit gain variation over frequency and temperature is shown in Figure 55. Overall gain variation should be between 52 and 63 dB (straight limit lines). Maximum and minimum measured gains of 62 dB and 57.34 dB, respectively, are recorded. Maximum gain variation over temperature of 3.23 dB, and maximum gain variation over frequency of 2.77 dB, over full 500 MHz band (29.5 to 30 GHz), are measured.

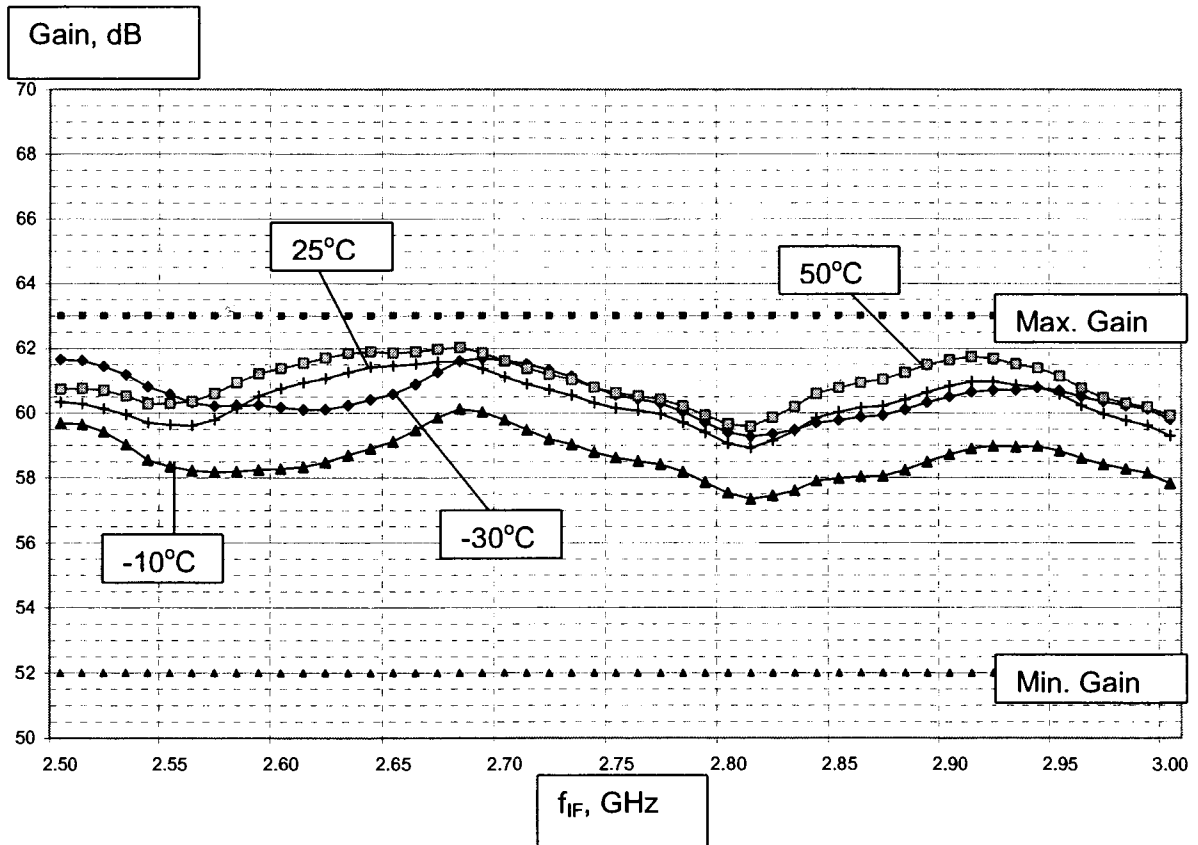


Figure 55: Measured transmitter gain variation over frequency and temperature.

Figure 56 illustrates input-versus-output power at 50 °C. Power of the input IF signal at 2.75 GHz is swept from -49.5 dBm to -23.5 dBm. Output RF signal at 29.75 GHz saturated power of +33 dBm is recorded. Measurement is performed at +50 °C ambient temperature since that is the worst-case condition for power amplifier operation (lowest unit gain – highest input level).

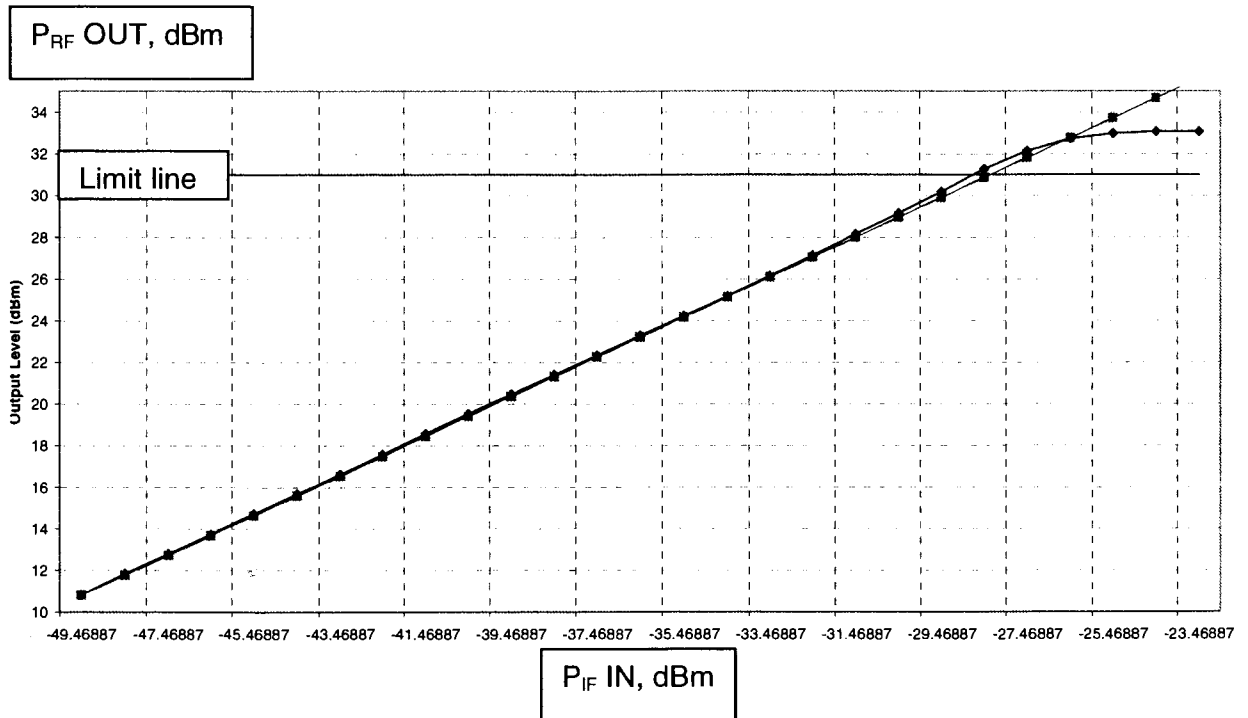


Figure 56: Measured transmitter input-versus-output power response at 50 °C ambient temperature.

Single side band (SSB) phase noise response for frequency offsets from 100Hz to 1MHz from the carrier, is presented in Figure 57. Phase noise of -87 dBc/Hz at 1 KHz offset (15 dB margin), -91 dBc/Hz at 10 KHz (9dB margin) and -98.5 dBc/Hz at 100 KHz offset (6.5 dB margin), is measured. Measurement is performed at 25°C ambient temperature, with 29.75 GHz output signal frequency.

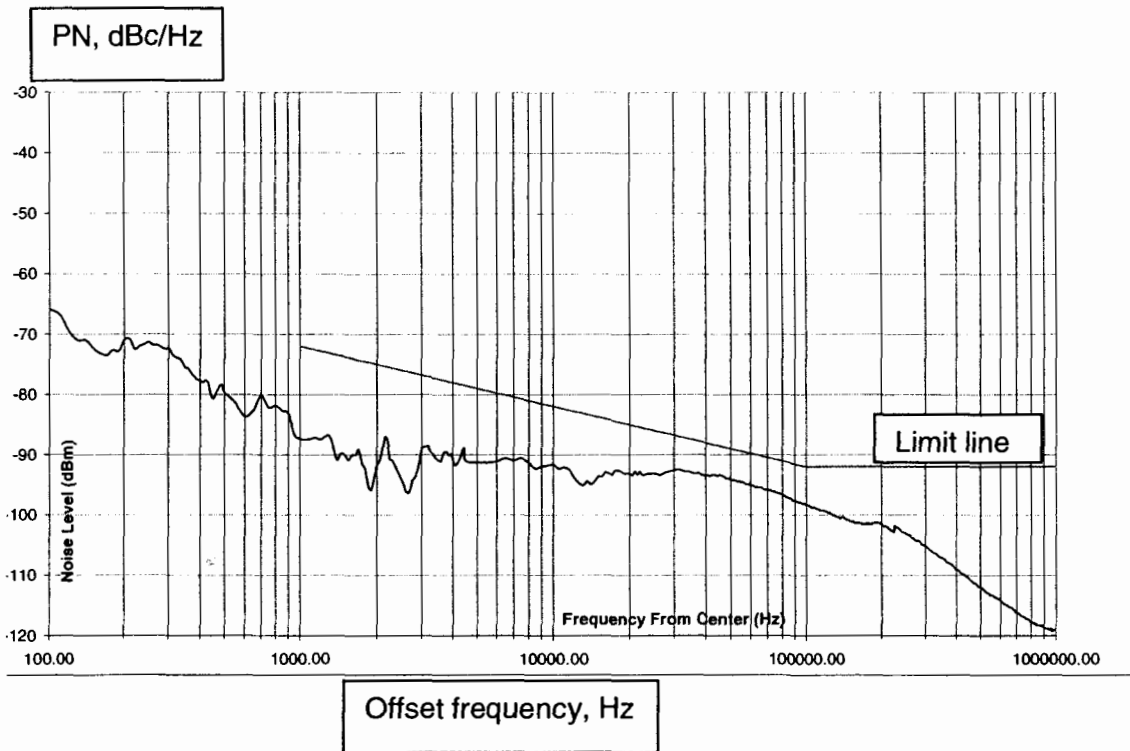


Figure 57: Measured transmitter phase noise response as a function of the offset frequency from carrier.

Figure 58 shows RF output power spectrum as a function of frequency. No in-band or out of band spurious signals are recorded. Measurement is performed at $-30\text{ }^{\circ}\text{C}$ ambient temperature since that is the worst-case condition for unit spurious content (highest unit gain – highest 2LO signal leakage).

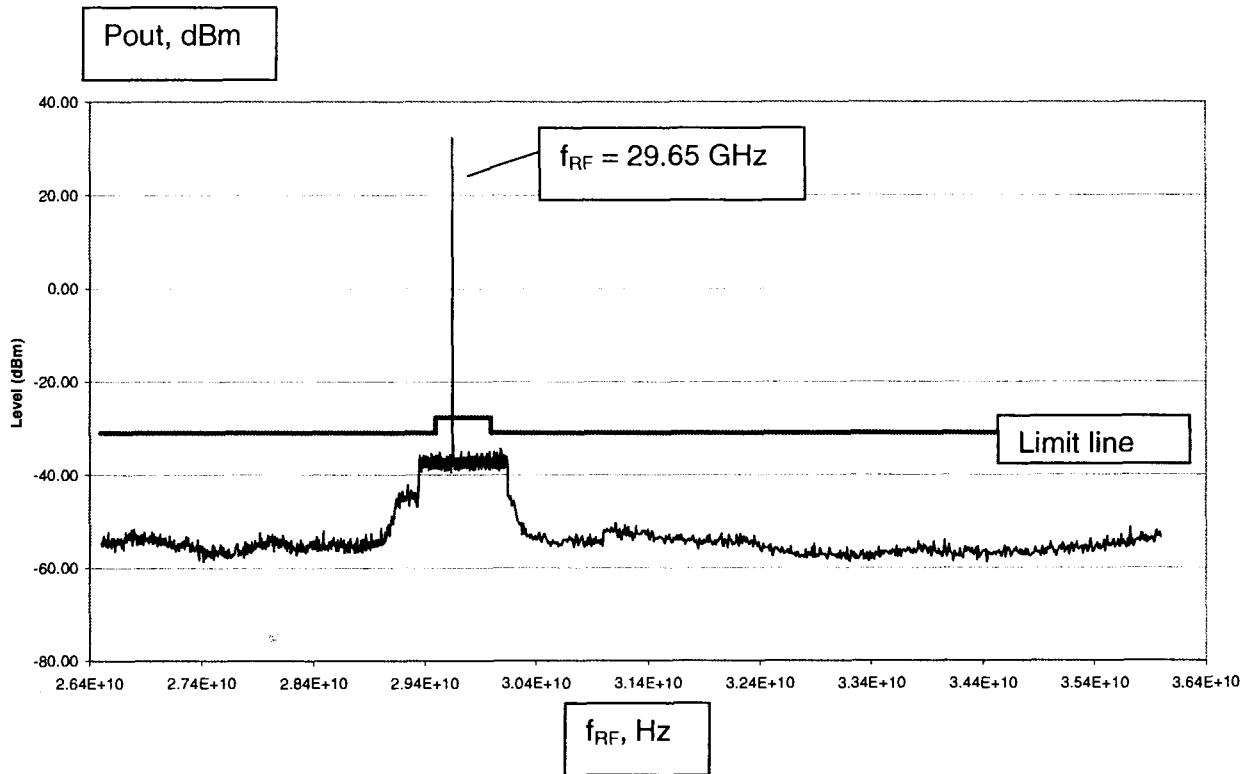


Figure 58: Measured transmitter output power spectrum as a function of frequency at $-30\text{ }^{\circ}\text{C}$ ambient temperature.

Table 6 presents part of the automatically generated measurement report. It should be noted that the unit exceeds specifications on all parameters with a considerable margin.

Table 6: Measurement results collected using automated measurement setup.

	Test Description	Spec.	Results	Comment
7	Operational Temperature Test			
	Power Consumption	$\leq 35\text{W}$	25.95W	[X] PASS [] FAIL
	Gain Variation Over Frequency			
	In any 20 MHz Band	$\leq 1\text{ dB}$	0.88dB	[X] PASS [] FAIL
	In Full 500 MHz Band	$\leq 5\text{dB}$	2.77dB	[X] PASS [] FAIL
	Max Gain	$\leq 63\text{dB}$	62.00dB	[X] PASS [] FAIL
	Min Gain	$\geq 52\text{dB}$	57.34dB	[X] PASS [] FAIL
	Gain Variation over Temperature	$\leq 6\text{dB}$	3.23dB	[X] PASS [] FAIL
	Saturation Point	$\geq 31.3\text{dBm}$	33.07dBm	[X] PASS [] FAIL
	Phase Noise @			
	1KHz/ 10KHz/ 100KHz	$\leq -72/ -82/ -92$ dBc/Hz	< -72/ -82/ -92dBc/Hz	[X] PASS [] FAIL
	Spurious Content			
	In Band	$\geq 60\text{ dBc}$	> 60dBc	[X] PASS [] FAIL
	Out of Band	$\leq -31\text{ dBm}$	< -31dBm	[X] PASS [] FAIL
	RF Off	$\leq -40\text{ dBm}$	< -40dBm	[X] PASS [] FAIL
	In Band Noise Emissions	$\leq -95\text{dBm/Hz}$	-99.92dBm/Hz	[X] PASS [] FAIL
	Frequency Stability over Temperature (referenced to 25° C.)	$\leq \pm 10\text{ppm}$	-7.03ppm	[X] PASS [] FAIL
	Hot Start		[X] PASS [] FAIL	
	Cold Start		[X] PASS [] FAIL	

4 RETURN CHANNEL LINK BUDGET CALCULATION

The measurements results presented in Section 3 demonstrated the actual Transmitter performance. Using these results, an ASTRA BBI RCS link budget calculation is performed, to evaluate system performance using a Norsat ODU.

4.1 Introduction

The Return Channel link is the communication path from the information source, through SIT to satellite (uplink), and from satellite, through the hub receiver, to the information sink (downlink).

For the chosen modulation scheme, the desired probability of error can be achieved only if sufficient signal to noise ratio is presented at the input of the receiver.

As discussed by Skalar [17], the goal of a link analysis is to determine whether or not the required probability of error performance is met. Since some of the budget parameters are statistical, analysis estimates available Carrier-to-Noise ratio or C/N. The difference between estimated and required C/N represents the safety margin.

4.2 Link Budget

Figure 59 depicts Ka-band, return channel link.

Paris, France (Longitude 2.3 deg. East, Latitude 48.8 deg. North) is chosen as a SIT site. Uplink frequency of 29.92 GHz is selected. This signal is picked up by ASTRA 1H GEO satellite Ka transponder (France beam; see Figure 8), positioned at 19.2 deg East. At the satellite, the signal is translated to 20.12 GHz frequency and beamed down to the BBI Hub. The Hub installation is located in Betzdorf, Luxemburg (Longitude 6 deg. East, Latitude 49.7 deg. North).

The calculation is performed for both a clear sky case, and a rain case. Paris and Betzdorf are both part of CCIR Rain Climate Zone E (from CCIR Recommendation 837) with 0.3% rain rate exceeded = 2.4mm/h.

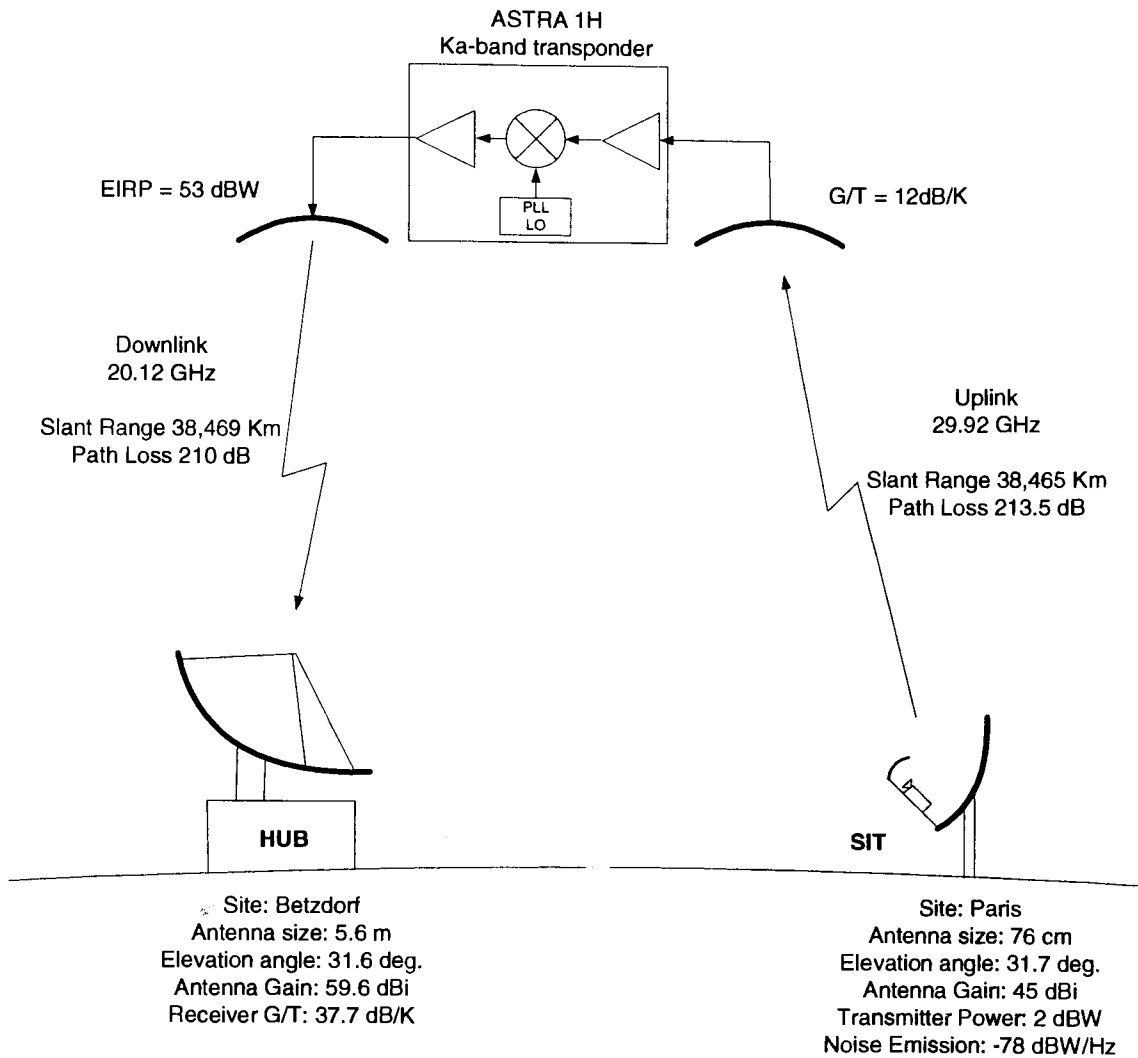


Figure 59: Return channel link between terminal located in Paris, France and hub located at Betzdorf, Luxemburg, over Ka-band satellite ASTRA 1H.

Table 7: Link budget calculation for clear sky and 0.3% rain rate exceeded conditions.

Parameter		Uplink @29.92 GHz		Downlink @ 20.12 GHz			
		Site: Paris		Site: Betzdorf			
			Clear Sky	Rain		Clear Sky	Rain
1.	Transmitter (Tx) Power	dBW	2	2			
2.	Output Back-off	dB	0	0		-31.7	-34.8
3.	Tx/Antenna Interface Loss	dB	-0.5	-0.5			
4.	Antenna Gain	dBi	45	45			
5.	EIRP	dBW	46.5	46.5		53	53
6.	Antenna Pointing Loss	dB	-0.3	-0.3		-0.7	-0.7
7.	Free Space Path Loss	dB	-213.5	-213.5		-210	-210
8.	Rain Loss	dB	0	-3		0	-1.2
9.	Atmosferic Absorption	dB	-0.5	-0.5		-0.5	-0.5
10.	Receiver G/T	dB/K	12	12		37.7	37
11.	Carrier C/T	dBW/K	-155.8	-158.8		-152.2	-157.2
12.	Bolctzmann's constant	dBW/K-Hz	-228.6	-228.6		-228.6	-228.6
13.	C/No	dB-Hz	72.8	69.8		76.4	71.4
14.	Xpol Interference C/lo	dB-Hz	84	81		74.9	74.9
	SIT Noise Interference C/lo						
15.	10K simultaneous users	dB-Hz	83	80			
16.	Adjacent Channel Interference C/lo	dB-Hz	77.9	74.9			
17.	Transponder Intermodulation C/lo					75	75
18.	Total Interference C/lo	dB-Hz	76.0	73.0		71.9	71.9
19.	Up-link C/(No+Io)	dB-Hz	71.1	68.1			
20.	Down-link C/(No+Io)	dB-Hz				70.6	68.7
21.	Available (Total Link) C/(No+Io)	dB-Hz	67.8	65.4			
22.	Available (Total Link) C/(N+I)	dB	9.9	7.4			
23.	BER Objective		1.00E-10				
24.	QPSK uncoded Eb/No	dB	13.2				
25.	Coding Gain	dB	9.5				
	Inner Convolutional 1/2 K=7						
	Outer Block RS(204,188,8)						
26.	Required Eb/No	dB	3.7				
27.	Implementation margin	dB	0.8				
28.	System margin	dB	1.9				
29.	Required C/N	dB	6.0				
30.	Margin		3.9	1.4			

The link budget calculation for Ka-band return link path, in ASTRA BBI network, is illustrated in Table 2.

As discussed in the literature [17, 18], carrier-to-noise power density (C/N_o) equation for uplink and downlink can be expressed as

$$C/N_o = EIRP - OBO - L_p + G/T - k \quad [dB-Hz]$$

Effective Isotropic Radiated Power (EIRP) is calculated as

$$EIRP = P_t - L_i + G_a \quad [dBW]$$

where P_t is transmitter output power [dBW],

L_i is loss due to feed cable [dB],

G_a is antenna gain [dBi],

Satellite manufacturer specifies EIRP for satellite downlink

OBO represents output amplifier back-off [dB].

L_p is space loss – decrease in signal strength due to the distance between the satellite and an Earth station. This is the largest signal loss in the link.

$L_p = (4 * \pi * d/\lambda)^2$; where d is slant distance and λ is wavelength at transmission frequency.

Other losses that are degrading link quality are:

- Antenna Pointing Loss is loss due to the transmitter or receiver antenna not being optimally pointed. Antenna gain pattern, as a function of pointing error angle, is given by

$$G_a = 29 - 25 * \log(\text{error angle}) \quad [dBi].$$

- Atmospheric absorption is loss due to oxygen and water vapor absorption.
- Rain is the main atmospheric cause for signal loss. To calculate rain loss, equations from reference [18] (1.20a and 1.20b) are used. Signal loss increases with rain intensity, due to absorption. In addition, the amount of noise radiated in to the receiver antenna (sky noise temperature), also increases with the rain intensity.

G/T is receiver antenna gain and system effective temperature (noise radiated into antenna and the thermal noise of the receiver front end) grouped together, sometimes called the receiver sensitivity.

k is Boltzmann's constant.

Another source of degradation in a satellite link is interference caused by unwanted signals injecting energy in the band of interest. The following interference sources are considered:

- Cross-polar Interference is characterized by an undesired signal appearing within the signal bandwidth due to inadequate discrimination between horizontal and vertical polarization by the antenna. Measured cross-polar level for the 76 cm antenna is 26 dB. Cross-polar performance of the hub's 5.6m antenna is estimated to be 17 dB.

$$C/I_o = C/I + 10 \log (\text{signal BW}) \quad [\text{dB-Hz}]$$

- SIT noise interference is a ratio between EIRP and noise spectral density at the SIT antenna output. For this type of SIT (type 2 – EIRP \geq 45 dBW) required NSD is -78 dBW/Hz. This interference is calculated with assumption that 10,000 users will simultaneously operate (per one beam).

$$C/I_o = \text{EIRP} - (\text{NSD} + 10 \log (\# \text{ of users})) \quad [\text{dB-Hz}]$$

- Adjacent Channel Interference is interference caused by energy spilling from an adjacent frequency channel, due to output stage nonlinearity (spectral regrowth). -20 dBc adjacent channel interference is present at the output of the SIT antenna when the terminal operates at specified EIRP level.
- Transponder Intermodulation is estimated to 17dB.

Uplink and Downlink carrier to noise and interference, is calculated using:

$$C/(N_o+I_o) = ((C/N_o)^{-1} + (C/I_o)^{-1})^{-1} \quad [\text{dB-Hz}]$$

The same formula is used when uplink and downlink ratios are combined to generate Available $C/(N_o+I_o)$.

Required C/N can be expressed as:

$$C/N \text{ req} = E_b/N_o - G_c + r \cdot R + M_i + M_s - BW \quad [\text{dB}]$$

E_b/N_o is bit energy per noise power spectral density, required to yield to desired bit error probability performance, without coding. As discussed in [19, 20] can be expressed as:

$$P = \text{BER} = 1/2 \operatorname{erfc}(\text{SQR}(E_b/N_o)) \quad \text{for QPSK (Gray encoded)}$$

G_c is coding gain and represents decrease in required E_b/N_o value, for same BER, due to coding implementation. Powerful concatenated code, formed of the outer Reed-Solomon RS(224, 188, 8) code and inner convolutional code rate 1/2 with constraints length 7, is applied to traffic and control data, to provide channel error

protection. The inner CC(2, 1, 7) Viterby soft decision decoder correct random errors. The errors at convolutional decoder output are bursty in nature, and outer RS code is used to correct them. ETSI EN 300 421 European standard document is specifying required Eb/No to 3.7 dB, for BER = 2×10^{-4} after Viterby and Quasi-Error-Free (QEF – corresponding to 10^{-10}) after Reed-Solomon decoder.

r is coding rate and R represents transmission rate. This calculation is performed for data rate of 384 Kbps (specified rate for SIT2) and symbol bandwidth of 0.618 MHz.

M_i stands for implementation margin, performance degradation due to the difference between the theoretical and the actual detection performance, caused by frequency offsets, timing errors and so on.

M_s corresponds to system margin, performance degradation due to imperfect synchronization reference.

BW is receiver noise bandwidth, and is equal to symbol rate.

The difference between available $C/(N+1)$ and required C/N represents *margin*.

A margin of 3.9 dB for clear sky condition, and 1.4 dB for rain with 0.3% rain rate exceeded, is the result of the link budget calculation.

The conclusion is that the Norsat transmitter/ODU deployed in ASTRA BBI network can yield to an availability of service equal to 99.7% for a transfer data rate of 348 Kbps.

5 CONCLUSION

Internet and multimedia applications have experienced tremendous growth in the last few years. Demand for high-speed access to widely dispersed servers is growing every day.

Among emerging mobile/wireless networks, geostationary Ka-band satellite networks, with their ability to deliver wide bandwidth independent of geography and local infrastructure, represent an ideal solution to handle this increasing demand.

The Ka-band transmitter, part of the satellite interactive terminal used for IP transfer over satellite, was reviewed. A detailed description of transmitters upconverter section, containing design considerations, block diagrams, schematics and simulation results, was conveyed. The measurement results matched very closely to simulation data. Unit level measurement results, obtained using an automated measurement system, illustrate that transmitter exceeds specification outlined by DVB-RCS standard, with a considerable margin on all parameters.

The return channel link budget calculation outlines that an availability of service equal to 99.7% at a data rate of 348 Kbps, can be achieved if the Norsat transmitter/ODU is deployed in the ASTRA BBI network.

Development work on new generation of Ka-transmitters, half the size and cost, is currently underway.

REFERENCES

- [1] ETSI Telecom Standards, <http://www.etsi.org/getastandard/home.htm> (accessed March 13, 2002).
- [2] Y. Zhang, D.D. Lucia, B. Ryu, and S. K. Dao, "Satellite Communications in the Global Internet: Issues, Pitfalls, and Potential," Hughes Research Laboratories, USA, http://www.iif.hu/rendezvenyek/inet97/F5/F5_1.HTM (accessed March 10, 2002).
- [3] Ka-band Report – Management Summary, <http://www.spotbeam.com> (accessed March 5, 2002).
- [4] J. Puetz, "Comparative Approaches in Implementing Wide Area Satellite Networks," *Pacific Telecommunication Conference*, Honolulu, Hawaii, January 1997.
- [5] ASTRA Satellites – The Footprints, <http://www.astra.lu/satellites/footprints.shtml#> (accessed March 15, 2002).
- [6] Eutelsat HotBird 6 satellite Information, <http://www.eutelsat.com/satellites/13ehb6.html#> (accessed March 15, 2002).
- [7] EuroSkyWay Network Information, <http://www.euroskyway.it/> (accessed March 15, 2002).
- [8] J. L. Fikart and A. Chan, "Outdoor Units for Ka/Ku-band Satellite Interactive Terminals," *Fifth Ka-band Utilization Conference Proceedings*, Taormina, Italy, Oct. 1999, pp. 437–444.
- [9] J. L. Fikart, "Outdoor Units For Ka/Ku-Band Satellite Interactive Terminals," *IEEE MTT-S International Microwave Symposium Digest*, 2001, vol. 2, pp. 1141–1144.
- [10] A. I. Zverev, *Handbook of Filter Synthesis*. New York: John Wiley and Sons, 1967, Chapter 4, pp. 107-136.
- [11] Ansoft Design Environment, <http://www.ansoft.com/products/hf/serenade/index.cfm> (accessed March 20, 2002).
- [12] Sirenza Microdevices Gain Blocks, http://www.sirenza.com/products/function/gain_blocks.html (accessed March 20, 2002)
- [13] A. Williams, *Electronic Filter Design Handbook*. New York: McGraw-Hill Book Company, 1981, pp. 8-12 to 8-15.
- [14] S. A. Maas, "A GaAs MESFET Mixer with Very Low Intermodulation," *IEEE Transaction on MTT*, April 1987, vol. MTT-35, no. 4, pp. 425–429.

- [15] NEC – CEL products, http://www.cel.com/prod/prod_smallsig.asp (accessed March 20, 2002).
- [16] Hittite Microwave Corporation – Mixer Products, http://www.hittite.com/index.cfm?body_content=products&type=mixer&catid=4&sort=function&source=leftnav (accessed March 20, 2002).
- [17] B. Skalar, *Digital Communications- Fundamentals and Applications*. New Jersey: Prentice Hall, 1988, pp. 188-240.
- [18] V. K. Bhargava, D. Haccoun, R. Matyas, and P. P. Nuspl, *Digital Communications by Satellite*. New York: John Wiley and Sons, 1981, pp. 10-28.
- [19] R. Steele, *Mobile Radio Communications*. London: Pentech Press, 1992, Chapter 4, pp. 347-484.
- [20] J. G. Proakis, *Digital Communications*, New York: McGraw-Hill, 1995, pp. 506-510.